

Dealing with Non-Stationarity in Multi-Agent Reinforcement Learning via Trust Region Decomposition

Wenhai Li[¶] Xiangfeng Wang[†] Bo Jin[†] Junjie Sheng[¶] Hongyuan Zha^{*}

Abstract

Non-stationarity is one thorny issue in multi-agent reinforcement learning, which is caused by the policy changes of agents during the learning procedure. Current works to solve this problem have their own limitations in effectiveness and scalability, such as centralized critic and decentralized actor (CCDA), population-based self-play, modeling of others and etc. In this paper, we novelly introduce a δ -stationarity measurement to explicitly model the stationarity of a policy sequence, which is theoretically proved to be proportional to the joint policy divergence. However, simple policy factorization like mean-field approximation will mislead to larger policy divergence, which can be considered as trust region decomposition dilemma. We model the joint policy as a general Markov random field and propose a trust region decomposition network based on message passing to estimate the joint policy divergence more accurately. The Multi-Agent Mirror descent policy algorithm with Trust region decomposition, called **MAMT**, is established with the purpose to satisfy δ -stationarity. MAMT can adjust the trust region of the local policies adaptively in an end-to-end manner, thereby approximately constraining the divergence of joint policy to alleviate the non-stationary problem. Our method can bring noticeable and stable performance improvement compared with baselines in coordination tasks of different complexity.

1 Introduction

Multi-agent system (MAS) exists in many real decision-making problems, such as multi-player games (Berner et al., 2019; Vinyals et al., 2019; Ye et al., 2020), resource allocation and network routing (Zimmer et al., 2020; Mao et al., 2020), where multiple agents learn and make decision together in a common environment, and can be solved by popular multi-agent reinforcement learning (MARL) algorithms. In addition, various practical applications like image segmentation (Liao et al., 2020), natural language processing (Feng et al., 2018) and recommendation systems (He et al., 2020) have been also modeled as the MAS.

Although deep RL has achieved great success in single-agent environments in recent years, MARL still has many additional challenges due to the complicated interaction among agents. This paper focuses on one of the thorny issues, i.e., the non-stationarity of MARL, which is caused by the changing of agents' policies during learning procedure. In a partially observable stochastic game (POSG), the state transition function T_i and the reward function R_i of agent i depend on the joint action \mathcal{A} of all agents. Because of the changing of its policy, each agent is urging T_j and R_j of each other agent j to change. Recently, many works have been proposed to deal with this non-stationary problem. These

[¶]School of Computer Science and Technology, East China Normal University, Shanghai, China. Email addresses: {52194501026, 52194501003}@stu.ecnu.edu.cn.

[†]School of Computer Science and Technology, East China Normal University and Shanghai Research Institute for Intelligent Autonomous Systems, Shanghai, China. Email addresses: {xfwang, bjin}@cs.ecnu.edu.cn.

^{*}School of Data Science, The Chinese University of Hong Kong(Shenzhen) and Shenzhen Institute of Artificial Intelligence and Robotics for Society, Shenzhen, China. Email address: zhahy@cuhk.edu.cn.

works can be roughly divided into two categories (Papoudakis et al., 2019): targeted modifications on some standard RL methods’ learning schemes (Lowe et al., 2017; Foerster et al., 2018b; Iqbal & Sha, 2019; Baker et al., 2019), or opponent information computing&sharing (Foerster et al., 2017; Raileanu et al., 2018; Foerster et al., 2018a; Rabinowitz et al., 2018; Al-Shedivat et al., 2018).

Both categories aim to mitigate the negative impact of policy changes to solve the non-stationary problem. However, because the definition of stationarity(or non-stationarity) is still lacking, the goals and objectives of these algorithms are inevitably inconsistent and disharmony, which make them ineffective. Meantime, these methods require either unextendable training scheme or excessive information exchanging, which significantly limits the algorithm scalability. If the policies of all agents change slowly, T_i and \mathcal{R}_i can remain stable. In this case, each agent could obtain the best-response to other agents, which will alleviate the non-stationary problem. An important class of RL algorithms usually limits the divergence between consecutive policies of learnt policy sequence by adding direct constraints or regularization terms. These methods are referred to as *trust region-based* or *proximity-based* algorithms (Schulman et al., 2015, 2017; Tomar et al., 2020). This motivates us to restrict the joint policy divergence to solve the non-stationary problem. However, the connection between joint policy divergence and the non-stationarity is still unclear, which drive us to theoretically analyze the relationship. Furthermore, for a MAS, directly adding the trust region constraint to the *joint* policy will make the problem intractable. Therefore, factorizing the joint policy and trust region constraint appropriately is the key to improve algorithm’s efficiency (Oliehoek et al., 2008).

In this paper, we first explicitly model the stationarity of the MARL algorithm learning procedure, and then propose a formal definition called δ -stationarity to measure the stationarity of a given policy sequence. Further, the proportional relationship between δ -stationarity and the joint policy divergence is theoretically established. This provides theoretical support to impose the trust region constraint on the learning procedure in order to alleviate the non-stationary problem. However, directly dealing with the trust region constraint on the joint policy will encounter computational complexity problems. Instead, we model the joint policy as a general Markov random field, and propose a trust region decomposition network based on message passing to factorize the trust region of the joint policy adaptively. After decomposition, local trust region constraints are imposed to all agents’ local policies, which can be efficiently solved through the mirror descent. The proposed algorithm is denoted as **Multi-Agent Mirror descent policy optimization with Trust region decomposition**, i.e., **MAMT**. MAMT can not only alleviate the non-stationary problem, but also transform the trust region constraint on the joint policy into trust region constraints on local policies, which could greatly improve the learning effectiveness and scalability.

Our contributions mainly consist of the following folds: 1) To our knowledge, this is the first measurement of the stationarity in MARL, with a well-established connection with the joint policy divergence. This proportional relationship can not only provide the theoretical support, but also deduce tractable learning algorithms; 2) The novel trust region decomposition scheme based on message passing and mirror descent, could approximately satisfy the δ -stationarity through a computationally efficient way; 3) Our proposed algorithm could bring noticeable and stable performance improvement in multiple coordination tasks of different complexity compared with baselines.

The following is the road-map of this paper. In Section 2 we provide a brief but comprehensive introduction to related works in non-stationarity and trust region, and provide the background material on cooperative POSG and the mirror descent method in Section 3. Section 4 explicitly model the stationarity of learning procedure and build the connection with the joint policy divergence. We present our algorithms and analyze them from various aspects in Section 5. Extensive experiments are presented in Section 6, and we conclude this paper in Section 7.

2 Related Works

2.1 Tackle Non-Stationarity in MARL

Many works have been proposed to tackle non-stationarity in MARL. These methods range from using a modification of standard RL training schemes to computing and sharing additional other agents' information. One modification of the standard RL training schemes is the centralized critic and decentralized actor (CCDA) architecture. Since the information of all other agents can be accessed by the centralized critics during training, the dynamics of the environment remain stable for the agent. [Lowe et al. \(2017\)](#) combined DDPG ([Lillicrap et al., 2016](#)) with CCDA architecture and proposed MADDPG algorithm. [Foerster et al. \(2018b\)](#) proposed a counterfactual baseline in the advantage estimation and used the REINFORCE ([Williams, 1992](#)) algorithm as the backbone in the CCDA architecture. Similar with [Lowe et al. \(2017\)](#), [Iqbal & Sha \(2019\)](#) combined SAC ([Haarnoja et al., 2018](#)) with CCDA architecture and introduced attention mechanism into the centralized critic design. In addition, [Iqbal & Sha \(2019\)](#) also introduced the counterfactual baseline proposed by [Foerster et al. \(2018b\)](#). CCDA alleviated of non-stationary problems indirectly makes it unstable and ineffective, and our experiments have also verified this.

Another modification to handle non-stationarity in MARL is self-play for competitive tasks or population-based training for cooperative tasks ([Papoudakis et al., 2019](#)). [Tesauro \(1995\)](#) used self-play to train the TD-Gammon which managed to win against the human champion in Backgammon. [Baker et al. \(2019\)](#) extended self-play to more complex environments with continuous state and action space. [Liu et al. \(2019\)](#) and [Jaderberg et al. \(2019\)](#) combined population-based training with self-play to solve complex team competition tasks, a popular 3D multiplayer first-person video game, *Quake III Arena Capture the Flag*, and *MuJoCo Soccer*, respectively. However, such methods require a lot of hardware resources and a well-designed parallelization platform.

In addition to modifying the standard RL training scheme, there are also methods to solve non-stationary problems by computing and sharing additional information. [Foerster et al. \(2017\)](#) proposed importance sampling corrections to adjust the weight of previous experience to the current environment dynamic to stabilize multi-agent experience replay. [Raileanu et al. \(2018\)](#) and [Rabinowitz et al. \(2018\)](#) used additional networks to predict the actions or goals of other agents, and input them as additional information into the policy network to assist decision-making. [Foerster et al. \(2018a\)](#) accessed the optimized trajectory of other agents by explicitly predicting the parameter update of other agents when calculating the policy gradient, thereby alleviating the non-stationary problem. These methods of explicitly considering other agents' information are also called *modeling of others*. Recently, [Al-Shedivat et al. \(2018\)](#) transformed non-stationary problems into meta-learning problems, and extended MAML ([Finn et al., 2017](#)) to MAS to find an initialization policy that can quickly adapt to non-stationarity. However, due to the special training mechanism of the above methods, they are difficult to extend to the tasks of more than 2 agents.

2.2 Trust Region Methods

Trust region or *proximity-based* methods, resonating the fact the they make the new policy to lie within a trust-region around the old one. Such methods include traditional dynamic programming-based conservative policy iteration (CPI) algorithm ([Kakade & Langford, 2002](#)), as well as deep RL methods, such as trust-region policy optimization (TRPO) ([Schulman et al., 2015](#)) and proximal policy optimization (PPO) ([Schulman et al., 2017](#)). TRPO used line-search to ensure that the KL divergence between the new policy and the old policy is below a certain threshold. PPO is to solve a more relaxed unconstrained optimization problem, in which the ratio of the old and new policy is clipped to a specific bound. [Wu et al. \(2017\)](#) (ACKTR) extended the framework of natural policy gradient and

proposed to optimize both the actor and the critic using Kronecker-factored approximate curvature (K-FAC) with trust region. [Nachum et al. \(2018\)](#) proposed an off-policy trust region method, Trust-PCL, which introduced relative entropy regularization to maintain optimization stability while exploiting off-policy data. Recently, [Tomar et al. \(2020\)](#) used mirror descent to solve a relaxed unconstrained optimization problem and achieved strong performance. Few works have introduced trust-region into MARL. [Li & He \(2020\)](#) transformed the multi-agent trust-region problem into a distributed consistency optimization problem, and proposed a decentralized method to stabilize the MARL training process. However, all agents have the same trust region and this will make the algorithm face the trust region decomposition dilemma.

3 Preliminaries

Cooperative POSG. POSG ([Hansen et al., 2004](#)) is denoted as a seven-tuple via the stochastic game (or Markov game)

$$\langle \mathcal{I}, \mathcal{S}, \{\mathcal{A}_i\}_{i=1}^n, \{\mathcal{O}_i\}_{i=1}^n, \mathcal{P}, \mathcal{E}, \{\mathcal{R}_i\}_{i=1}^n \rangle,$$

where n denotes the number of agents; \mathcal{I} represents the agent space; \mathcal{S} represents the finite set of states; $\mathcal{A}_i, \mathcal{O}_i$ denote a finite action set and a finite observation set of agent $i \in \mathcal{I}$ respectively; $\mathcal{A} = \mathcal{A}_1 \times \mathcal{A}_2 \times \dots \times \mathcal{A}_n$ is the finite set of joint actions; $\mathcal{P}(s'|s, \mathbf{a})$ denotes the Markovian state transition probability function, where $s, s' \in \mathcal{S}$ represent states of environment and $\mathbf{a} = \{a_i\}_{i=1}^n, a_i \in \mathcal{A}_i$ represents the action of agent i ; $\mathcal{O} = \mathcal{O}_1 \times \mathcal{O}_2 \times \dots \times \mathcal{O}_n$ is the finite set of joint observations; $\mathcal{E}(\mathbf{o}|s)$ is the Markovian observation emission probability function, where $\mathbf{o} = \{o_i\}_{i=1}^n, o_i \in \mathcal{O}_i$ represents the local observation of agent i ; $\mathcal{R}_i : \mathcal{S} \times \mathcal{A} \times \mathcal{S} \rightarrow \mathcal{R}$ denotes the reward function of agent i and $r_i \in \mathcal{R}_i$ is the reward of agent i . The game in POSG unfolds over a finite or infinite sequence of stages (or timesteps), where the number of stages is called *horizon*. In this paper, we consider the finite horizon case. The objective for each agent is to maximize the expected cumulative reward received during the game. For a cooperative POSG, we quote the definition in [Song et al. \(2020\)](#),

$$\forall i \in \mathcal{I}, \forall i' \in \mathcal{I} \setminus \{i\}, \forall \pi_i \in \Pi_i, \forall \pi_{i'} \in \Pi_{i'}, \frac{\partial \mathcal{R}_{i'}}{\partial \mathcal{R}_i} \geq 0,$$

where i and i' are a pair of agents in agent space \mathcal{I} ; π_i and $\pi_{i'}$ are the corresponding policies in the policy space Π_i and $\Pi_{i'}$ respectively. Intuitively, this definition means that there is no conflict of interest for any pair of agents.

Mirror descent method in RL. The mirror descent method ([Beck & Teboulle, 2003](#)) is a typical first-order optimization method, which can be considered as an extension of the classical proximal gradient method. In order to minimize the objective function $f(\mathbf{x})$ under a constraint set $\mathbf{x} \in \mathcal{C} \subseteq \mathbb{R}^n$, the basic iterative scheme at iteration $k+1$ can be written as

$$\mathbf{x}^{k+1} \in \arg \min_{\mathbf{x} \in \mathcal{C}} \langle \nabla f(\mathbf{x}^k), \mathbf{x} - \mathbf{x}^k \rangle + \gamma^k B_\psi(\mathbf{x}, \mathbf{x}^k), \quad (1)$$

where $B_\psi(\mathbf{x}, \mathbf{y}) := \psi(\mathbf{x}) - \psi(\mathbf{y}) - \langle \nabla \psi(\mathbf{y}), \mathbf{x} - \mathbf{y} \rangle$ denotes the Bregman divergence associated with a strongly convex function ϕ and γ^k is the step size (or learning rate). Each reinforcement learning problem can be formulated as optimization problems from two distinct perspectives, i.e.,

$$\pi^*(\cdot | s) \in \arg \max_{\pi} V^\pi(s), \quad \forall s \in \mathcal{S}; \quad (2a)$$

$$\pi^* \in \arg \max_{\pi} \mathbb{E}_{s \sim \mu}[V^\pi(s)]. \quad (2b)$$

[Geist et al. \(2019\)](#) and [Shani et al. \(2020\)](#) have utilized the mirror descent scheme (1) and update the policy iteratively as follows

$$\begin{aligned}\pi^{k+1}(\cdot|s) &\leftarrow \arg \max_{\pi} \mathbb{E}_{a \sim \pi} [A^{\pi^k}(s, a)] - \gamma^k \text{KL}(\pi, \pi^k); \\ \pi^{k+1} &\leftarrow \arg \max_{\pi} \mathbb{E}_{s \sim \rho_{\pi^k}} [\mathbb{E}_{a \sim \pi} [A^{\pi^k}(s, a)] - \gamma^k \text{KL}(\pi, \pi^k)],\end{aligned}$$

where $\text{KL}(\cdot, \cdot)$ denotes the Bregman divergence corresponding to negative entropy function.

4 The Stationarity of the Learning Procedure

To explore and mitigate the non-stationarity in MARL, we first need to explicitly model the stationarity or non-stationarity. To emphasize, the non-stationarity is not an inherent attribute of a POSG itself, but is additionally introduced when using a specific learning algorithm (e.g., MARL) to solve the POSG. Therefore, we propose the following definition on stationarity for the obtained policy sequence in the learning procedure.

Definition 1 (δ -stationarity of the learning procedure). *For a MAS containing n agents, a joint policy sequence $\{\pi_{\psi^0}, \dots, \pi_{\psi^t}, \dots\}$ will be generated during the learning procedure, where the joint policy is parameterized by ψ^t at step t . The action of agent i at state s is denoted as a_i , while the joint action of all other agents is denoted a_{-i} . The joint policy of other agents $\pi_{\psi_{-i}^t}$ is parameterized by ψ_{-i}^t at step t . If the joint policy of the other agents changes from $\pi_{\psi_{-i}}$ to $\pi_{\psi'_{-i}}$, the transition probability from current joint observation \mathbf{o} to next joint observation \mathbf{o}' of agent i will change from $p(\mathbf{o}'|\mathbf{o}, a_i)$ to $q(\mathbf{o}'|\mathbf{o}, a_i)$ with*

$$\begin{aligned}p(\mathbf{o}'|\mathbf{o}, a_i) &= \int p(\mathbf{o}'|\mathbf{o}, a_i, a_{-i}) \pi_{\psi_{-i}}(a_{-i}|\mathbf{o}) da_{-i}, \\ q(\mathbf{o}'|\mathbf{o}, a_i) &= \int p(\mathbf{o}'|\mathbf{o}, a_i, a_{-i}) \pi_{\psi'_{-i}}(a_{-i}|\mathbf{o}) da_{-i}, \\ p(\mathbf{o}'|\mathbf{o}, a_i, a_{-i}) &= \int p(\mathbf{o}'|s') p(s'|\mathbf{o}, a_i, a_{-i}) ds'.\end{aligned}$$

If for any two consecutive policies $\pi_{\psi_{-i}^t}$ and $\pi_{\psi_{-i}^{t+1}}$, we have

$$D_{\text{KL}}(p(\mathbf{o}'|\mathbf{o}, a_i) \| q(\mathbf{o}'|\mathbf{o}, a_i)) \leq \delta_i, \quad \forall \mathbf{o}, \mathbf{o}', a_i,$$

then the learning procedure of agent i is δ_i -stationary. Further, if all agents are δ -stationary with corresponding $\{\delta_i\}$, then the learning procedure of entire multi-agent system is δ -stationary with $\delta = \frac{1}{n} \sum_i \delta_i$.

The above definition is a direct mathematical description of the non-stationary problem ([Hernandez-Leal et al., 2017](#); [Papoudakis et al., 2019](#)), which can essentially measure the non-stationarity of the learning procedure. However, the above definition is still far from being utilized to design an achievable algorithm. Therefore, exploring the relationship between δ -stationarity and policies is a crucial step to transform the above definition into an algorithm friendly scheme. Moreover, in the δ -stationarity definition, policies occupy an important part. It is intuitive and reasonable to explicitly establish the connection between non-stationarity and policies. The following theorem aims to establish the connection between δ -stationarity and the divergence of the joint policy of other agents.

Theorem 1. *For any agent i , the divergence of its transition probability distribution has the following relationship with the divergence of the joint policy of other agents, i.e.,*

$$D_{\text{KL}}(p(\mathbf{o}'|\mathbf{o}, a_i) \| q(\mathbf{o}'|\mathbf{o}, a_i)) \propto D_{\text{KL}}(\pi_{\psi_{-i}}(\mathbf{o}) \| \pi_{\psi'_{-i}}(\mathbf{o})).$$

Due to the proportional relationship between the transition probability distribution divergence of the agent and the divergence of the joint policy of the other agents, according to Definition 1, we can control the non-stationarity of the MAS by constraining the joint policy divergence of the other agents. The trust region-based RL algorithms usually constrain the policy divergence, while for each agent we can also impose a trust region constraint on the joint policy of the other agents. As a result, the non-stationarity of the entire MAS can be further controlled. However, computing the joint policy divergence of the other agents $D_{\text{KL}}(\pi_{\psi_{-i}}(\mathbf{o}) \parallel \pi_{\psi'_{-i}}(\mathbf{o}))$ in Theorem 1 still has high computational complexity. For a MAS with n agents, n constraints on the joint policy divergence should be modeled simultaneously. Before proposing the algorithm, we still need to relax the constraints on the joint policy divergence, with the purpose to increase effectiveness and scalability. Base on the following theorem, the constraints on the joint policy divergence of the other agents can be limited by the joint policy divergence of all agents, which could be independent of the agent number. Both detailed proofs of Theorem 1 and the following Theorem 2 can be found in appendix.

Theorem 2. *For a multi-agent system, the divergence of the all agents' joint policy is the upper bound of the average divergence of other agents' joint policy*

$$\frac{1}{n} \sum_{i=1}^n D_{\text{KL}}(\pi_{\psi_{-i}}(a_{-i}|\mathbf{o}) \parallel \pi_{\psi'_{-i}}(a_{-i}|\mathbf{o})) \leq D_{\text{KL}}(\pi_\psi(\mathbf{a}|\mathbf{o}) \parallel \pi_{\psi'}(\mathbf{a}|\mathbf{o})).$$

With the above Theorem 2, we only need to impose only one trust region constraint on all agents' joint policy to control the non-stationarity of the entire learning procedure. This allows us to obtain a MARL algorithm with good effectiveness and scalability to approximate δ -stationarity.

5 The Proposed MAMT Algorithm

According to Theorem 2, we need to limit the divergence of joint policy to make the learning procedure more stable. But this will cause learning dilemma to complete the task if we try to completely eliminate the non-stationarity (i.e., $\delta = 0$). If $\delta = 0$, the joint policy of all agents could not be updated. To emphasize, based on Definition 1, Theorem 1 and Theorem 2, we can modify the original MARL problem model by adding stationarity constraint, i.e.,

$$\begin{aligned} \pi^{k+1} &\in \arg \max_{\pi} \mathbb{E}_{\mathbf{o} \sim \mu} \left[\sum_{i=1}^n V_i^\pi(\mathbf{o}) \right], \\ \text{s.t. } \mathbb{E}_{\mathbf{o} \sim \mu} \left[D_{\text{KL}}(\pi(\cdot|\mathbf{o}), \pi^k(\cdot|\mathbf{o})) \right] &\leq \varepsilon, \end{aligned} \tag{4}$$

where π represents the joint policy of all agents; $\mathbf{o} := (o_1, \dots, o_i, \dots, o_n)$ represents the joint observation with n be the agent number. However, directly imposing a constraint on the joint policy as in (4) will make the problem significantly more difficult and computationally intractable. Inspired by Lowe et al. (2017), Foerster et al. (2018b) and Iqbal & Sha (2019), we introduce the *Mean-Field approximation* assumption in this paper.

Assumption 1 (Mean-Field Approximation). *We use the mean-field variation family π to estimate the joint policy of all agents*

$$\pi(\mathbf{a}|\mathbf{o}) = \prod_{i=1}^n \pi_i(a_i|o_i). \tag{5}$$

Based on mean-field approximation assumption, the joint policy trust region constraint can be factorized into trust region constraints of local policies with the following theorem.

Theorem 3. For any consecutive policies which are belong to mean-field variational family π and π^k in the policy sequence obtained by any learning algorithm, the KL divergence constraint on joint policy in (4) is equivalent with the following summation constraints of local policies, i.e.,

$$\sum_{i=1}^n \mathbb{E}_{o_i \sim \mu_i} [D_{\text{KL}}(\pi_i(\cdot|o_i), \pi_i^k(\cdot|o_i))] \leq \varepsilon. \quad (6)$$

Further the joint summation trust region constraint (6) can be equivalently decomposed into the following local trust region constraints, i.e.,

$$\mathbb{E}_{o_i \sim \mu_i} [D_{\text{KL}}(\pi_i(\cdot|o_i), \pi_i^k(\cdot|o_i))] \leq \varepsilon_i, \quad \forall i, \quad (7)$$

with $\sum_{i=1}^n \varepsilon_i = \varepsilon$, $0 \leq \varepsilon_i \leq \varepsilon$; π_i and π_i^k represent the consecutive local policies of agent i ; o_i and u_i represent the local observation and initial local observation distribution of agent i respectively.

Due to the summation constraint term (6), it is still need to jointly train the policies of all agents with limited effectiveness and scalability. As a result, we further equivalently transform (6) into (7), which is proposed to constraint each agent's local policy separately[¶].

5.1 MAMD: Multi-Agent Mirror Descent Policy Optimization

Based on the results in [Theorem 3](#), problem (4) can be reformulated as

$$\begin{aligned} \pi^{k+1} &\in \arg \max_{\pi} \mathbb{E}_{\mathbf{o} \sim \mu} \left[\sum_{i=1}^n V_i^{\pi}(\mathbf{o}) \right], \\ \text{s.t. } \mathbb{E}_{o_i \sim \mu_i} [&D_{\text{KL}}(\pi_i(\cdot|o_i), \pi_i^k(\cdot|o_i))] \leq \frac{\varepsilon}{n}, \quad \forall i. \end{aligned} \quad (8)$$

By directly combing the general algorithm framework of MAAC ([Iqbal & Sha, 2019](#)) and the mirror descent technique in MDPO ([Tomar et al., 2020](#)), we can obtain the fundamental *Multi-Agent Mirror Descent Policy Optimization*(MAMD) algorithm framework. Each agent i has its local policy network π_{ψ_i} and a local critic network Q_{ζ_i} , which is similar with MADDPG ([Lowe et al., 2017](#)). All critics are centralized updated iteratively by minimizing a joint regression loss function, i.e.,

$$\mathcal{L}_{\text{critic}}(\zeta_1, \dots, \zeta_n) = \sum_{i=1}^n \mathbb{E}_{(o, a, r, o') \sim \mathcal{D}} \left[(Q_{\zeta_i}(o, a) - y_i)^2 \right], \quad (9)$$

with

$$y_i = r_i + \gamma \mathbb{E}_{a' \sim \pi_{\psi}(o')} [Q_{\bar{\zeta}_i}(o', a') - \alpha \log(\pi_{\psi_i}(a'_i | o'_i))],$$

and the parameters of the attention module are shared among agents; $\pi_{\bar{\psi}}$ represents the joint target policy (similar as target Q -network in DQN) of all agents; $Q_{\bar{\zeta}_i}$ represents the target local critic of agent i . α denotes the temperature balancing parameter between maximal entropy and rewards. As for the individual policy updating step, the mirror descent technique ([Tomar et al., 2020](#)) is introduced to deal with the decomposed local trust region constraints in (8). The policy gradient is calculated with the following form:

$$\nabla_{\psi_i} J(\pi_{\psi}) = \mathbb{E}_{o \sim \mathcal{D}, a \sim \pi} \left[\nabla_{\psi_i} \log(\pi_{\psi_i}(a_i | o_i)) \left(\frac{\text{KL}[\theta_i || \theta_i^{\text{old}}]}{\varepsilon_i} + Q_{\zeta_i}(o, a) - b(o, a_{\setminus i}) \right) \right], \quad (10)$$

[¶]In this case, the number of constraints will increase to n , however the number of constraints will become n^2 if the decomposition technique is imposed on the n joint policy of the other agents.

where $b(o, a_{\setminus i})$ denotes the counterfactual baseline (Foerster et al., 2018b); $\pi_{\theta_i^{\text{old}}}$ represents the policy of agent i at last step; ε_i is the assigned trust-region range; $\text{KL}[\theta_i \parallel \theta_i^{\text{old}}] = \log(\pi_{\theta_i}(a_i | o_i)) - \log(\pi_{\theta_i^{\text{old}}}(a_i | o_i))$. However, if we only perform a single-step SGD the resulting gradient would be equivalent to vanilla policy gradient and misses the entire purpose of enforcing the trust-region constraint. As a result, the policy update at each iteration k involves m SGD steps as

$$\begin{aligned}\psi_{i,k}^{(0)} &= \psi_{i,k}, \quad j = 0, \dots, m-1; \\ \psi_{i,k}^{(j+1)} &\leftarrow \psi_{i,k}^{(j)} + \eta \nabla_{\psi_i} J(\pi_\psi) \Big|_{\psi_i=\psi_{i,k}^{(j)}}, \quad \psi_{i,k+1} = \psi_{i,k}^{(m)}.\end{aligned}$$

For off-policy mirror descent policy optimization, performing multiple SGD steps at each iteration becomes increasingly time-consuming as the value of m grows. Therefore, similar with Tomar et al. (2020), we resort to staying close to an m step old copy of the current policy, while performing a single gradient update at each iteration of the algorithm. This copy is updated every m iterations with the parameters of the current policy. MAMD approximately constrains the joint policy divergence by evenly decompose the trust region constraint onto the local policies. The pseudo-code of MAMD are shown in appendix.

5.2 Trust Region Decomposition Dilemma

The trust region decomposition scheme adopted in the above MAMD is based on mean-field approximation assumption(i.e., formulation (8)). However, decomposing trust region inappropriately will make the algorithm converge to sub-optimal solutions, which can be numerically proved through the following example. By considering a simple MAS with of three agents i, j, k , we assume that the agent k is independent with other two agents i and j . Then for the multi-agent system, we have

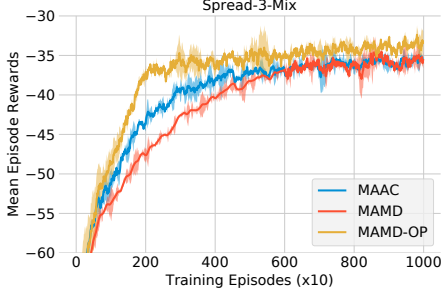
$$\begin{aligned}p_i(\mathbf{o}' | \mathbf{o}, a_i, a_j, a_k) &= p_i(\mathbf{o}' | \mathbf{o}, a_i, a_j), \\ p_j(\mathbf{o}' | \mathbf{o}, a_j, a_i, a_k) &= p_j(\mathbf{o}' | \mathbf{o}, a_j, a_i), \\ p_k(\mathbf{o}' | \mathbf{o}, a_k, a_i, a_j) &= p(\mathbf{o}' | \mathbf{o}, a_k).\end{aligned}\tag{11}$$

The change of agent k 's policy cannot affect the state transition probability of i and j , and vice versa. As a result, the constraints on the agent i and agent j are “insufficient” but the constraint for agent k is “excessive”, when we decompose the trust region ε in (6) into three parts equally, i.e., $\varepsilon/3$. This phenomenon is called *trust region decomposition dilemma* in this paper. To numerically verify the existence of this dilemma, the performance comparison of MAMD in the variant *Spread* environment with different trust region decomposition schemes is proposed in Figure 1a. **MAMD-OP** represents only the same trust region constraint on the agent i and j . More details can be found in appendix. It is obvious in Figure 1a that inappropriate decomposition can even bring performance degradation.

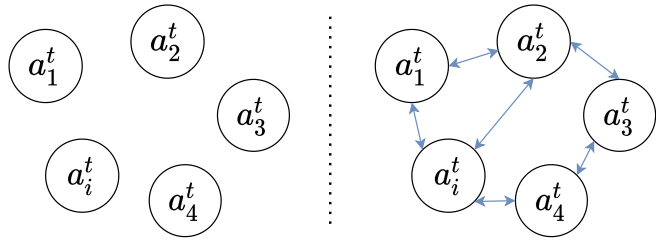
Theoretically, the reason for the trust region decomposition dilemma might be the inaccurately estimation of the joint policy divergence based on mean-field approximation assumption. The simple summation of local policies' divergence is not equal to the divergence of the joint policy, while the gap might be enormous. Once the joint policy divergence cannot be accurately estimated, we cannot judge the non-stationarity of the current learning procedure, and imposing constraints on it may run counter to our goals. In order to effectively solve the trust region decomposition dilemma, we propose the following framework.

5.3 The MAMT Algorithm Framework

To achieve more reasonable decomposition of joint policy, some recent works (Böhmer et al., 2020; Qu et al., 2020; Li et al., 2020) modeled the joint policy as a general Markov random field (as shown in



(a) Performance.



(b) Probabilistic graphical models.

Figure 1: (a) Performance comparisons of different decomposition schemes; (b) The probabilistic graphical models of two different modelings of the joint policy. **Left:** Modeling the joint policy with the mean-field variation family; **Right:** Modeling the joint policy as a general Markov random field. Each node represents the action of agent i at timestep t .

the Figure 1b). Further graph neural networks (GNNs) are usually employed to simulate the message passing (or belief propagation). Inspired by these methods, a similar mechanism is utilized in this paper to estimate the divergence of the joint policy. Further the joint policy divergence is related to the current local policies of all agents and the trust regions of agents' local policies, which all can be input to the GNN. To emphasize, we can appropriately decompose the trust region in a end-to-end procedure by minimizing the modeled divergence of the joint policy. The employed graph neural networks is denoted as *trust region decomposition network* and the network structure is shown in Figure 2.

However, two important issues need to be properly solved to guarantee an implementable and tractable algorithm. For the reason that the divergence of joint policy cannot be directly calculated, a surrogate is needed as the supervision signal to train trust region decomposition network; Furthermore, since the dependence between agents is an important factor affecting the calculation of joint policy divergence as discussed in Section 5.2, we need to reasonably model the dependencies between agents. In the following, we will solve these problems in a targeted way and propose our MAMT algorithm framework. MAMT uses the trust region decomposition network to estimate the joint policy divergence more accurately. At the same time, the trust region sizes of the local policies are adaptively adjusted by the trade-off between minimizing joint policy divergence and maximizing accumulated reward, thereby solving the trust region decomposition dilemma.

Improved Joint Policy Divergence Approximation. Instead of directly calculating the joint policy divergence with summation of local policy divergences, we estimate the divergence terms through the trust region decomposition network. The trust region decomposition network need to be learned based on some supervised information, which can be obtained by an well-defined indicator of non-stationarity. As discussed before, the non-stationary problem is caused by dynamic changing of the other agents' policies, which leads to the out-of-distribution of sampled data from the environment. As a result, we borrowed the idea in offline RL to measure the degree of out-of-distribution through the model-based RL (Kidambi et al., 2020; Yu et al., 2020), with the purpose to reasonably characterize the non-stationarity. Specifically, each agent i has a prediction model $h_{\phi_i^j}$ for each other agent j , which can predict the other agents' actions based on its local observation. The summation of the divergence between the predicted action distribution and the real action distribution of all other agents could represent the degree of non-stationarity of the agent i , i.e.,

$$\mathcal{D}_{i,\text{ns}}^t = \Pi_{\text{ns}} \left(\sum_{j \neq i} \mathcal{C}_{i,j}^t \left(\text{KL} \left[h_{\phi_i^j}(o_i^t) \| \pi_{\psi_j}(o_j^t) \right] \right) \right), \quad (12)$$

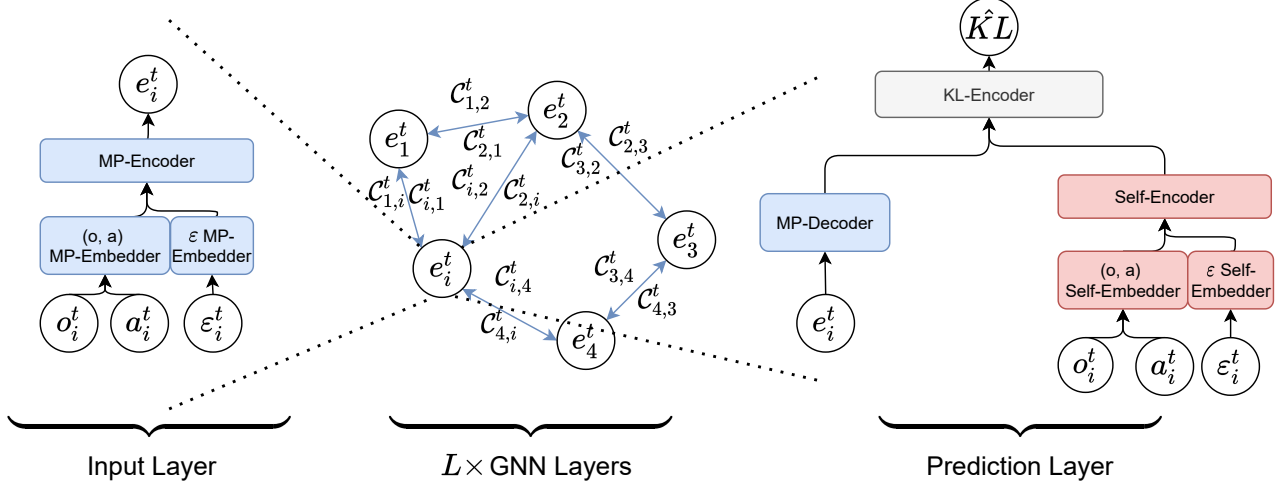


Figure 2: The architecture of trust region decomposition network. “MP” denotes message passing. At each timestep t , each agent i first encodes its local observation o_i^t and action a_i^t , and concatenates them with the embedding of the local trust-region coefficient (a trainable parameter), and finally gets the agent’s embedding from the MP-Encoder output. Next, we construct all agents as a weighted undirected graph, the weights $C_{*,*}^t$ are calculated in advance, and the updated agent’s embedding is obtained through graph convolution. At the same time, similar to the input layer, each agent obtains the another agent’s embedding through another neural network with the same structure but different parameters. Finally, we concatenate the two embeddings together and input them into KL-Encoder to obtain an estimation of the the current joint policy divergence.

where “ns” denotes the “non-stationarity”; t represents the current timestep; $C_{i,j}^t$ is the coordination coefficient (we will explain soon) between agent i and agent j ; π_{ψ_j} is the policy of agent j which is parameterized by ψ_j ; Π_{ns} represents the projection function, which constrains $\mathcal{D}_{i,\text{ns}}^t$ to a specific range to stabilize the training procedure. Furthermore, the non-stationarity of MAS can be denoted as the summation of all local non-stationarities, i.e.,

$$\mathcal{D}_{\text{ns}}^t = \sum_i \mathcal{D}_{i,\text{ns}}^t,$$

which can be considered as the supervised signal for trust region decomposition network training. The loss function to learn the trust region decomposition network can be formulated as

$$\min_{\theta} \mathcal{L}_{\text{ns}} = \left(\sum_i \hat{KL}_i^t - \sum_i \mathcal{D}_{i,\text{ns}}^t \right)^2, \quad (13)$$

where θ and \hat{KL}_i^t are the parameters and the output of the trust region decomposition network respectively.

Calculation of Coordination Coefficient. We use a non-negative real number, coordination coefficient, to represent the dependency between two agents[†]. In the actual MAS learning procedure, the coordination relationship between agents is changing with the learning of policies and the completion of tasks. Therefore, we model the cooperative relationship between two agents based on counterfactual (Foerster et al., 2018b; Jaques et al., 2019). In Jaques et al. (2019), the causal influence reward of

[†]In this paper, we only model the pairwise relationship.

agent i w.r.t. opponent j is calculated by

$$c_{i,j}^t = D_{KL} \left[p(a_j^t | a_i^t, o_j^t) \| p(\tilde{a}_j^t | o_j^t) \right],$$

where $p(a_j^t | s_j^t) = \sum_{\tilde{a}_i^t} p(a_j^t | \tilde{a}_i^t, o_j^t) p(\tilde{a}_i^t | o_j^t)$. It can be seen that the greater the causal influence reward, the tighter the coordination between the two agents, so this reward value can be used as the coordination coefficient. However, when calculating the causal influence reward, the agent's policy needs to be modified, that is, the agent needs to explicitly rely on the actions of other agents when making decisions. To solve this problem, we modified the process of calculating the counterfactual baseline in [Foerster et al. \(2018b\)](#) based on the idea of [Jaques et al. \(2019\)](#), and obtained a new way of calculating the coordination coefficient

$$\begin{aligned} \hat{C}_{i,j} &= \text{softmax} \left(\left| Q_i(\mathbf{a}_{\setminus j}) - Q_i(\mathbf{a}) \right| \right), \\ C_{i,j} &= \begin{cases} \hat{C}_{i,j}, & \hat{C}_{i,j} \geq \delta, \\ 0, & \hat{C}_{i,j} \leq \delta, \end{cases} \end{aligned} \quad (14)$$

where $Q_i(\cdot)$ is the centralized critic of agent i . \mathbf{a} is the joint action of all agents and $\mathbf{a}_{\setminus j}$ is the joint action of all agents except for j ; δ is the threshold to keep sparsity.

The MAMT ALgorithm Framework. In this section, we propose our **M**ulti-**A**gent **M**irror descent policy algorithm with Trust region decomposition, i.e., MAMT. The framework of MAMT is established based on MAMD, while the improved joint policy divergence approximation driven trust region decomposition network is employed. Furthermore, the local trust region parameter ε_i of each agent i also need to be transparently learned adaptively, rather than pre-defined as in MAMD. The learning of ε_i involves the mutual balance of two parts, i.e. the non-stationarity of the learning procedure and the performance of all agents. The objective of ε_i learning is to maximize

$$\mathcal{F}(\varepsilon) := \mathbb{E}_{\mathbf{o} \sim \mu} \left[\sum_{i=1}^n V_i^{\pi(\varepsilon)}(\mathbf{o}) - \hat{KL}_i^{\pi(\varepsilon)}(\mathbf{o}, \varepsilon; \theta) \right],$$

where $\varepsilon = \{\varepsilon_i\}_{i=1}^n$ and $\pi(\varepsilon)$ represent the joint policy is related to the local trust regions ε_i of all agents; $\hat{KL}_i^{\pi(\varepsilon)}$ denotes the output of trust region decomposition network which is parameterized by θ . Finally, the learning of $\{\varepsilon_i\}$ and θ can be modeled as a bilevel optimization problem

$$\begin{aligned} \varepsilon^* &= \arg \min \mathcal{F}(\varepsilon, \theta^*(\varepsilon)), \\ \text{s.t. } \theta^*(\varepsilon) &= \arg \min \mathcal{L}_{\text{ns}}(\varepsilon, \theta). \end{aligned}$$

We can employ the efficient two-timescale gradient descent method to simultaneously perform gradient update for both ε and θ . Specifically, we have

$$\begin{aligned} \varepsilon_{k+1} &\leftarrow \varepsilon_k - \alpha_k \cdot \nabla_{\varepsilon} \mathcal{F}(\varepsilon_k, \theta_k), \\ \theta_{k+1} &\leftarrow \theta_k - \beta_k \cdot \nabla_{\theta} \mathcal{L}_{\text{ns}}(\varepsilon_k, \theta_k), \text{ s.t. } \frac{\alpha_k}{\beta_k} \rightarrow 0, \end{aligned} \quad (15)$$

where $\frac{\alpha_k}{\beta_k} \rightarrow 0$ indicates that $\{\theta_k\}_{k \geq 0}$ updates in a faster pace than $\{\varepsilon_k\}_{k \geq 0}$. In practical implementation, we make α_k and β_k equal but perform more gradient descent steps on θ , similar as [Fujimoto et al. \(2018\)](#).

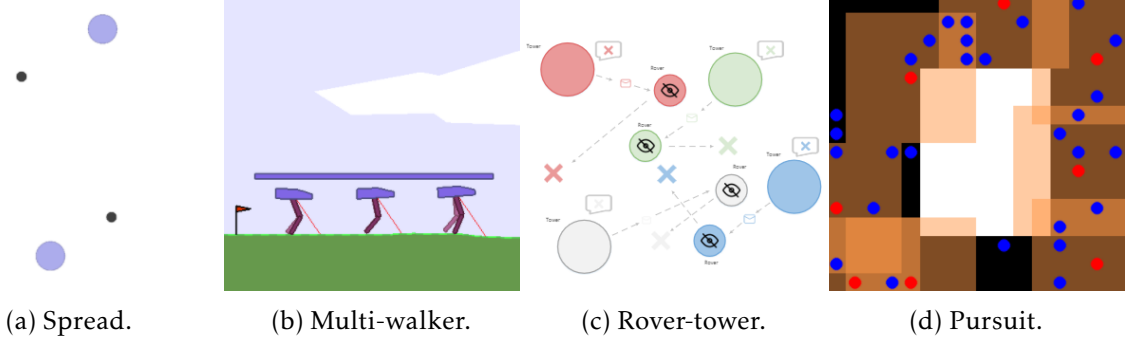


Figure 3: Coordination environments with increasing complexity.

6 Experiments

Our experiments aim to verify the effectiveness and scalability of the MAMT algorithm. The effectiveness of the trust region constraints on joint policy, the existence of trust region decomposition dilemma, and the capacity of the trust region decomposition will be discussed and proved from the point of view of experiment. Four coordination environments with increasing complexity, i.e. *Spread*, *Multi-Walker*, *Rover-Tower*, *Pursuit* (see Figure 3), are employed and detailed environment definitions are proposed in appendix.

Baseline Algorithms. **MADDPG**, which is one of the typical CCDA algorithms, is chosen as one baseline. The core of our proposed methods are the proposed trust region techniques, which motivates us to set the combination of PPO and MADDPG as another baseline and be labeled as **MA-PPO**. The **MAAC** is considered as the baseline, which is based on attention mechanism to modeling other agents. In addition, the **LOLA** algorithm that models opponent agents to solve the non-stationary problem is compared as baseline. Since LOLA employed the Taylor expansion to explicitly add the information of the opponents to the gradient, while the extension to more agents seems to be difficult and it is only compared in the *Spread* environment. To emphasize, the **MAMD** algorithm is also set to be the baseline.

Comparisons. we compare MAMT with all baselines and get the following three conclusions.

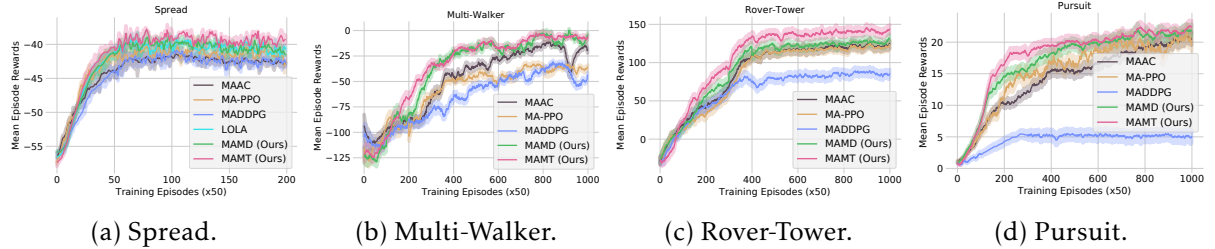


Figure 4: The performance comparisons under coordination tasks with different complexity.

1) *Combining the single-agent trust region technique with MARL directly cannot bring stable performance improvement.* The averaged episode rewards of our methods and baselines in four different coordination environments are shown in Figure 4. From the performance comparison of MAAC and MA-PPO, it can be seen that directly combining the single-agent trust region technique with MARL cannot bring stable performance improvement. In the *Rover-Tower* and *Pursuit*, MA-PPO did not bring noticeable improvement in final performance; MA-PPO only has a relatively noticeable and

stable performance improvement in the simple *Spread* environment, and even causes a performance degradation in *Multi-Walker*. In contrast, both MAMT and MAMD can bring noticeable and stable performance improvements in all environments.

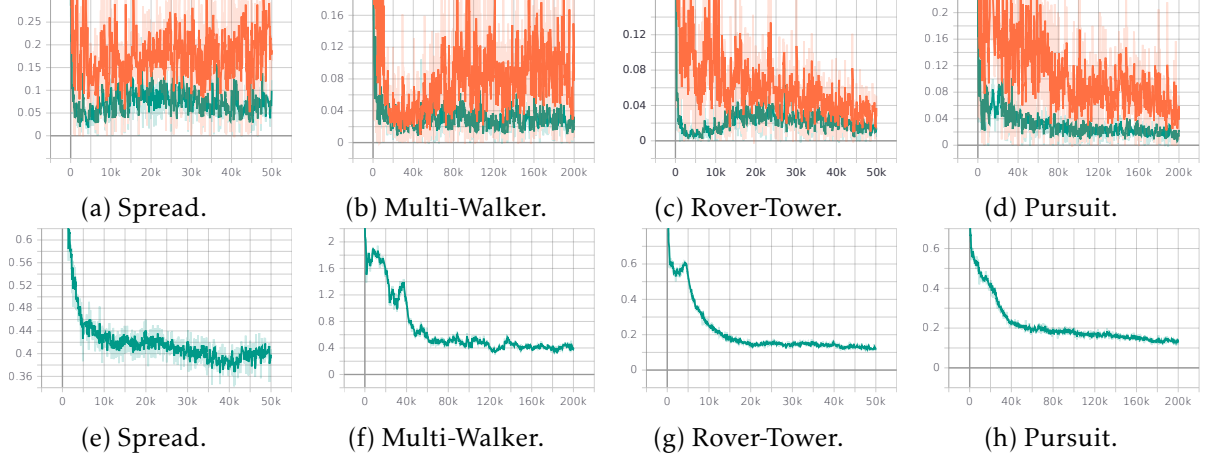


Figure 5: **Upper:** The averaged KL divergence of each agent with yellow and green line representing MAAC and MAMT respectively; **Bottom:** The \mathcal{D}_{ns} of all agents.

(2) MAMT achieves the trust region constraint on the local policies and minimizes the non-stationarity of the learning procedure. Below we conduct an in-depth analysis of the reasons why MAMT can noticeably and stably improve the final performance. MAMT use an end-to-end approach to adaptively adjust the sizes of the trust regions of the local policies according to the current dependencies between agents, so as to more accurately constrain the KL divergence of the joint policy. Therefore, we analyze MAMT from the two perspectives: the trust region constraint satisfaction of the local policies and the non-stationarity satisfaction via surrogate measure. Figure 5 shows the average value of the KL divergence of all agents' local policies during learning procedure in different environments. It can be seen from the figure that MAMT obviously controls the policy divergence. The non-stationarity of the learning procedure is difficult to calculate according to the definition, so we use the surrogate measure \mathcal{D}_{ns} to represents the non-stationarity. It can be seen from Figure 5 that as the learning progresses, the non-stationarity is gradually decreasing.

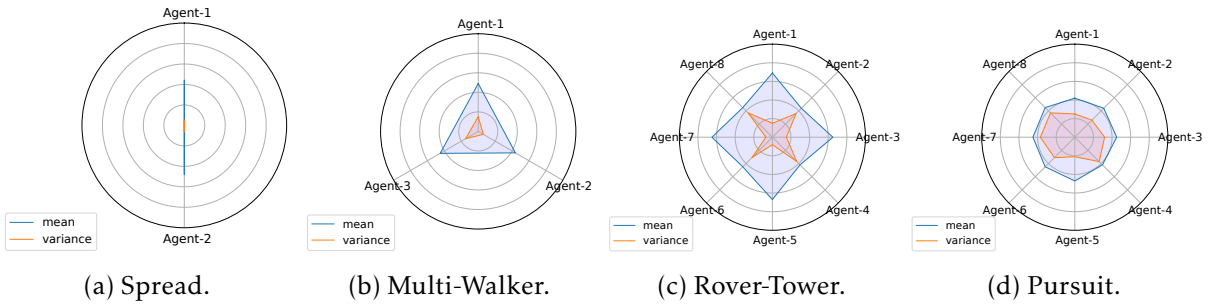


Figure 6: Mean and variance of local trust region of each agent in all environments. The y-axis range from 0.01 to 100.0.

(3) Trust region decomposition works better when there are more agents and more complex coordination relationships. It can be seen from Figure 4 that MAMT and MAMD have similar performance in the *Spread* and *Multi-Walker*, but MAMT is noticeably better than MAMD in the *Rover-Tower* and *Pursuit*. To analyze the reasons for this phenomenon, we separately record the coordination coefficients

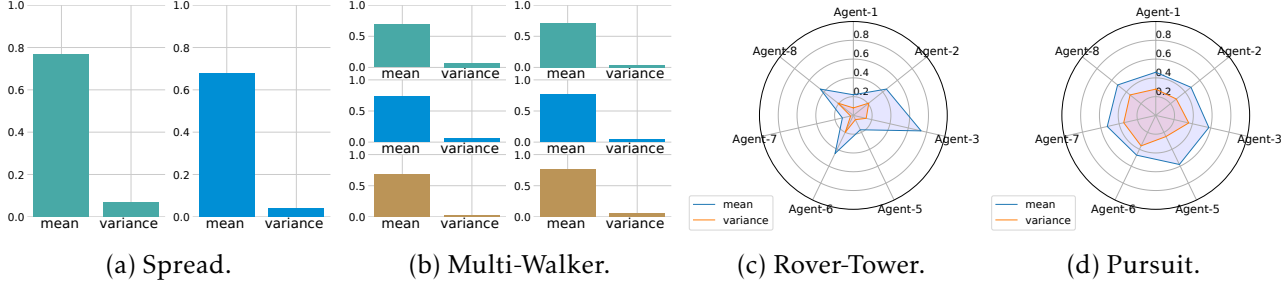


Figure 7: Mean and variance of coordination coefficients between all two agents in four coordination environments. Different colors represent different agents in (a) and (b). In addition, since there are fewer agents in *Spread* and *Multi-Walker*, the display effect of radar chart is poor, so we use histogram for a clearer display in (a) and (b).

between agents in the learning procedure, and the sizes of the trust regions of the local policies, see [Figure 7](#) and [Figure 6](#). It can be seen from [Figure 7](#) that because the *Spread* and *Multi-Walker* are relatively simple and the number of agents is small, the interdependence between agents is very tight (larger mean) and will not change over time (variance is very small). And the corresponding trust region sizes are similar as coordination coefficients. These figures show that in simple coordination tasks with a small number of agents, trust region decomposition is not a serious problem, which leads to the fact that the MAMT cannot bring a noticeable performance improvement. In other two environments, the dependence between agents is not static (the variance in [Figure 7](#) is larger) due to the larger number of agents and more complex tasks. This also makes the sizes of the trust regions of the agent’s local policies fluctuate greatly in different stages (the variance in [Figure 6](#) is larger). MAMT alleviates these impact of trust region decomposition dilemma through trust region decomposition network, which brings a noticeable and stable performance improvement.

7 Conclusion

In this paper, we define the δ -stationarity to explicitly model the stationarity in the learning procedure of the multi-agent system and provide a theoretical basis for proposing a achievable learning algorithm based on joint policy trust region constraints. To solve the trust region decomposition dilemma caused by the mean field approximation and to estimate the joint policy divergence more accurately, we propose an efficiency and scalable algorithm MAMT combining message passing and mirror descent with the purpose to satisfy δ -stationarity. Experiments show that MAMT can bring noticeable and stable performance improvement and more suitable for large-scale scenarios with complex coordination relationships between agents.

References

- Al-Shedivat, M., Bansal, T., Burda, Y., Sutskever, I., Mordatch, I., and Abbeel, P. Continuous adaptation via meta-learning in nonstationary and competitive environments. In *ICLR*, 2018.
- Baker, B., Kanitscheider, I., Markov, T., Wu, Y., Powell, G., McGrew, B., and Mordatch, I. Emergent tool use from multi-agent autocurricula. In *ICLR*, 2019.
- Beck, A. and Teboulle, M. Mirror descent and nonlinear projected subgradient methods for convex optimization. *Operations Research Letters*, 31(3):167–175, 2003.

- Berner, C., Brockman, G., Chan, B., Cheung, V., Debiak, P., Dennison, C., Farhi, D., Fischer, Q., Hashme, S., Hesse, C., Józefowicz, R., Gray, S., Olsson, C., Pachocki, J. W., Petrov, M., de Oliveira Pinto, H. P., Raiman, J., Salimans, T., Schlatter, J., Schneider, J., Sidor, S., Sutskever, I., Tang, J., Wolski, F., and Zhang, S. Dota 2 with large scale deep reinforcement learning. *ArXiv*, abs/1912.06680, 2019.
- Böhmer, W., Kurin, V., and Whiteson, S. Deep coordination graphs. In *ICML*, 2020.
- Feng, J., Li, H., Huang, M., Liu, S., Ou, W., Wang, Z., and Zhu, X. Learning to collaborate: Multi-scenario ranking via multi-agent reinforcement learning. In *WWW*, 2018.
- Finn, C., Abbeel, P., and Levine, S. Model-agnostic meta-learning for fast adaptation of deep networks. In *ICML*, 2017.
- Foerster, J., Chen, R. Y., Al-Shedivat, M., Whiteson, S., Abbeel, P., and Mordatch, I. Learning with opponent-learning awareness. In *AAMAS*, 2018a.
- Foerster, J. N., Nardelli, N., Farquhar, G., Afouras, T., Torr, P., Kohli, P., and Whiteson, S. Stabilising experience replay for deep multi-agent reinforcement learning. In *ICML*, 2017.
- Foerster, J. N., Farquhar, G., Afouras, T., Nardelli, N., and Whiteson, S. Counterfactual multi-agent policy gradients. In *AAAI*, 2018b.
- Fujimoto, S., Hoof, H., and Meger, D. Addressing function approximation error in actor-critic methods. In *ICML*, 2018.
- Geist, M., Scherrer, B., and Pietquin, O. A theory of regularized markov decision processes. In *ICML*, 2019.
- Haarnoja, T., Zhou, A., Abbeel, P., and Levine, S. Soft actor-critic: Off-policy maximum entropy deep reinforcement learning with a stochastic actor. In *ICML*, 2018.
- Hansen, E. A., Bernstein, D. S., and Zilberstein, S. Dynamic programming for partially observable stochastic games. In *AAAI*, 2004.
- He, X., An, B., Li, Y., Chen, H., Wang, R., Wang, X., Yu, R., Li, X., and Wang, Z. Learning to collaborate in multi-module recommendation via multi-agent reinforcement learning without communication. In *RecSys*, 2020.
- Hernandez-Leal, P., Kaisers, M., Baarslag, T., and de Cote, E. M. A survey of learning in multiagent environments: Dealing with non-stationarity. *arXiv preprint arXiv:1707.09183*, 2017.
- Iqbal, S. and Sha, F. Actor-attention-critic for multi-agent reinforcement learning. In *ICML*, 2019.
- Jaderberg, M., Czarnecki, W. M., Dunning, I., Marrs, L., Lever, G., Castaneda, A. G., Beattie, C., Rabinowitz, N. C., Morcos, A. S., Ruderman, A., et al. Human-level performance in 3d multiplayer games with population-based reinforcement learning. *Science*, 364(6443):859–865, 2019.
- Jaques, N., Lazaridou, A., Hughes, E., Gulcehre, C., Ortega, P., Strouse, D., Leibo, J. Z., and De Freitas, N. Social influence as intrinsic motivation for multi-agent deep reinforcement learning. In *ICML*, 2019.
- Kakade, S. and Langford, J. Approximately optimal approximate reinforcement learning. In *ICML*, 2002.

- Kidambi, R., Rajeswaran, A., Netrapalli, P., and Joachims, T. MOReL: Model-based offline reinforcement learning. In *NeurIPS*, 2020.
- Li, H. and He, H. Multi-agent trust region policy optimization. *arXiv preprint arXiv:2010.07916*, 2020.
- Li, S., Gupta, J. K., Morales, P., Allen, R., and Kochenderfer, M. J. Deep implicit coordination graphs for multi-agent reinforcement learning. *arXiv preprint arXiv:2006.11438*, 2020.
- Liao, X., Li, W., Xu, Q., Wang, X., Jin, B., Zhang, X., Zhang, Y., and Wang, Y. Iteratively-refined interactive 3D medical image segmentation with multi-agent reinforcement learning. In *CVPR*, 2020.
- Lillicrap, T. P., Hunt, J. J., Pritzel, A., Heess, N., Erez, T., Tassa, Y., Silver, D., and Wierstra, D. Continuous control with deep reinforcement learning. In *ICLR*, 2016.
- Liu, S., Lever, G., Merel, J., Tunyasuvunakool, S., Heess, N., and Graepel, T. Emergent coordination through competition. In *ICLR*, 2019.
- Lowe, R., Wu, Y., Tamar, A., Harb, J., Abbeel, O. P., and Mordatch, I. Multi-agent actor-critic for mixed cooperative-competitive environments. In *NeurIPS*, 2017.
- Mao, H., Liu, W., Hao, J., Luo, J., Li, D., Zhang, Z., Wang, J., and Xiao, Z. Neighborhood cognition consistent multi-agent reinforcement learning. In *AAAI*, 2020.
- Nachum, O., Norouzi, M., Xu, K., and Schuurmans, D. Trust-pcl: An off-policy trust region method for continuous control. In *ICLR*, 2018.
- Oliehoek, F. A., Spaan, M. T., and Vlassis, N. Optimal and approximate Q-value functions for decentralized POMDPs. *Journal of Artificial Intelligence Research*, 32:289–353, 2008.
- Papoudakis, G., Christianos, F., Rahman, A., and Albrecht, S. V. Dealing with non-stationarity in multi-agent deep reinforcement learning. *ArXiv*, abs/1906.04737, 2019.
- Qu, C., Li, H., Liu, C., Xiong, J., Zhang, J., Chu, W., Qi, Y., and Song, L. Intention propagation for multi-agent reinforcement learning. *arXiv preprint arXiv:2004.08883*, 2020.
- Rabinowitz, N., Perbet, F., Song, F., Zhang, C., Eslami, S. A., and Botvinick, M. Machine theory of mind. In *ICML*, 2018.
- Raileanu, R., Denton, E., Szlam, A., and Fergus, R. Modeling others using oneself in multi-agent reinforcement learning. In *ICML*, 2018.
- Schulman, J., Levine, S., Abbeel, P., Jordan, M., and Moritz, P. Trust region policy optimization. In *ICML*, 2015.
- Schulman, J., Wolski, F., Dhariwal, P., Radford, A., and Klimov, O. Proximal policy optimization algorithms. *arXiv preprint arXiv:1707.06347*, 2017.
- Shani, L., Efroni, Y., and Mannor, S. Adaptive trust region policy optimization: Global convergence and faster rates for regularized mdps. In *AAAI*, 2020.
- Song, Y., Wang, J., Lukasiewicz, T., Xu, Z., Xu, M., Ding, Z., and Wu, L. Arena: A general evaluation platform and building toolkit for multi-agent intelligence. In *AAAI*, 2020.

Terry, J. K., Black, B., Jayakumar, M., Hari, A., Santos, L., Dieffendahl, C., Williams, N. L., Lokesh, Y., Sullivan, R., Horsch, C., and Ravi, P. PettingZoo: Gym for multi-agent reinforcement learning. *arXiv preprint arXiv:2009.14471*, 2020.

Tesauro, G. Temporal difference learning and TD-Gammon. *Communications of the ACM*, 38(3):58–68, 1995.

Tomar, M., Shani, L., Efroni, Y., and Ghavamzadeh, M. Mirror descent policy optimization. *arXiv preprint arXiv:2005.09814*, 2020.

Vinyals, O., Babuschkin, I., Czarnecki, W., Mathieu, M., Dudzik, A., Chung, J., Choi, D., Powell, R., Ewalds, T., Georgiev, P., Oh, J., Horgan, D., Kroiss, M., Danihelka, I., Huang, A., Sifre, L., Cai, T., Agapiou, J. P., Jaderberg, M., Vezhnevets, A. S., Leblond, R., Pohlen, T., Dalibard, V., Budden, D., Sulsky, Y., Molloy, J., Paine, T. L., Gulcehre, C., Wang, Z., Pfaff, T., Wu, Y., Ring, R., Yogatama, D., Wünsch, D., McKinney, K., Smith, O., Schaul, T., Lillicrap, T., Kavukcuoglu, K., Hassabis, D., Apps, C., and Silver, D. Grandmaster level in StarCraft II using multi-agent reinforcement learning. *Nature*, pp. 1–5, 2019.

Williams, R. J. Simple statistical gradient-following algorithms for connectionist reinforcement learning. *Machine Learning*, 8(3-4):229–256, 1992.

Wu, Y., Mansimov, E., Grosse, R. B., Liao, S., and Ba, J. Scalable trust-region method for deep reinforcement learning using kronecker-factored approximation. In *NeurIPS*, 2017.

Ye, D., Chen, G., Zhang, W., Chen, S., Yuan, B., Liu, B., Chen, J., Liu, Z., Qiu, F., Yu, H., Yin, Y., Shi, B., Wang, L., Shi, T., Fu, Q., Yang, W., Huang, L., and Liu, W. Towards playing full MOBA games with deep reinforcement learning. In *NeurIPS*, 2020.

Yu, T., Thomas, G., Yu, L., Ermon, S., Zou, J., Levine, S., Finn, C., and Ma, T. MOPO: Model-based offline policy optimization. In *NeurIPS*, 2020.

Zimmer, M., Siddique, U., and Weng, P. Learning fair policies in decentralized cooperative multi-agent reinforcement learning. *ArXiv*, abs/2012.09421, 2020.

A Pseudo-code of MAMD

Algorithm 1: MAMD.

Input: initial behavior policy π_{ψ_i} and main centralized critic Q_{ζ_i} for each agent i , empty replay buffer \mathcal{D}

- 1 Set target critic $Q_{\bar{\zeta}_i}$ equal to main critic;
- 2 Set target policy $\pi_{\bar{\psi}_i}$ equal to behavior policy;
- 3 Set old policy $\pi_{\psi_i}^{\text{old}}$ equal to behavior policy;
- 4 **while** not convergence **do**
- 5 Observe local observation o_i and select action $a_i \sim \pi_\epsilon(\cdot | o_i)$ for each agent i ;
- 6 Execute joint action a in the environment;
- 7 Observe next local observation o'_i , local reward r_i and local done signal d_i of each agent i ;
- 8 Store $(\{o_i\}, \{a_i\}, \{r_i\}, \{o'_i\}, \{d_i\})$ in replay buffer \mathcal{D} ;
- 9 **if** All d_i are terminal **then**
- 10 Reset the environment;
- 11 **if** it's time to update **then**
- 12 **for** j in range(however many updates) **do**
- 13 Sample a batch of transitions \mathcal{B} from \mathcal{D} ;
- 14 Update centralized critic of all agents by Eq. 9;
- 15 Update individual policy of all agents by Eq. 10;
- 16 Update target networks $Q_{\bar{\zeta}_i}$ and $\pi_{\bar{\psi}_i}$;
- 17 **if** it's time to update **then**
- 18 Update old policy $\pi_{\psi_i}^{\text{old}}$;

B Pseudo-code of MAMT

Algorithm 2: MAMT

Input: initial behavior policy π_{ψ_i} and main centralized critic Q_{ζ_i} for each agent i , empty replay buffer \mathcal{D} , trust region decomposition network f_{θ_-} and g_{w_+} , local trust region ε_i^0

- 1 Set target critic $Q_{\bar{\zeta}_i}$ equal to main critic;
- 2 Set $\pi_{\bar{\psi}_i}$ and $\pi_{\psi_i}^{\text{old}}$ equal to behavior policy;
- 3 **while** not convergence **do**
- 4 Observe local observation o_i and select action $a_i \sim \pi_\varepsilon(\cdot | o_i)$ for each agent i ;
- 5 Execute joint action a in the environment;
- 6 Observe next local observation o'_i , local reward r_i and local done signal d_i of each agent i ;
- 7 Store $(\{o_i\}, \{a_i\}, \{r_i\}, \{o'_i\}, \{d_i\})$ in replay buffer \mathcal{D} ;
- 8 **if** it's time to update **then**
- 9 **for** j in range(however many updates) **do**
- 10 Sample a batch of transitions \mathcal{B} from \mathcal{D} ;
- 11 Compute $\{\mathcal{C}_{i,\setminus i}^t\}$ with Eq. 14;
- 12 Compute $\{\mathcal{D}_{i,\text{ns}}^t\}$ with Eq. 12;
- 13 **for** slow update **do**
- 14 Update ε_i^t with Eq. 15;
- 15 **for** fast update **do**
- 16 Update f_{θ_-}, g_{w_+} with Eq. 15;
- 17 Update centralized critic of all agents by Eq. 9;
- 18 Update individual policy of all agents by Eq. 10;
- 19 Update target networks $Q_{\bar{\zeta}_i}$ and $\pi_{\bar{\psi}_i}$;
- 20 **if** it's time to update **then**
- 21 Update old policy $\pi_{\psi_i}^{\text{old}}$;

C Proof of Theorem 3

Proof.

$$\begin{aligned}
& \mathbb{E}_{\mathbf{o} \sim \mu} [\text{KL}(\pi(\cdot|\mathbf{o}), \pi^k(\cdot|\mathbf{o}))] < \varepsilon \\
\iff & \mathbb{E}_{\mathbf{o} \sim \mu} \left[\int_a \pi(\cdot|\mathbf{o}) \log \frac{\pi(\cdot|\mathbf{o})}{\pi^k(\cdot|\mathbf{o})} da \right] < \varepsilon \\
\iff & \mathbb{E}_{\mathbf{o} \sim \mu} \left[\int_a \pi(\cdot|\mathbf{o}) \left(\sum_{i=1}^n \log \frac{\pi_i(\cdot|o_i)}{\pi_i^k(\cdot|o_i)} \right) da \right] < \varepsilon \\
\iff & \mathbb{E}_{\mathbf{o} \sim \mu} \left[\sum_{i=1}^n \int_a \pi(\cdot|\mathbf{o}) \log \frac{\pi_i(\cdot|o_i)}{\pi_i^k(\cdot|o_i)} da \right] < \varepsilon \\
\iff & \sum_{i=1}^n \mathbb{E}_{\mathbf{o} \sim \mu} \left[\int_a \pi(\cdot|\mathbf{o}) \log \frac{\pi_i(\cdot|o_i)}{\pi_i^k(\cdot|o_i)} da \right] < \varepsilon \\
\iff & \sum_{i=1}^n \left[\int_{\mathbf{o}} \mu(\mathbf{o}) \int_a \pi(\cdot|\mathbf{o}) \log \frac{\pi_i(\cdot|o_i)}{\pi_i^k(\cdot|o_i)} da d\mathbf{o} \right] < \varepsilon.
\end{aligned}$$

We first simplify the integral term of the inner layer

$$\begin{aligned}
& \int_a \pi(\cdot|\mathbf{o}) \log \frac{\pi_i(\cdot|o_i)}{\pi_i^k(\cdot|o_i)} da \\
\iff & \int_{a_{\setminus i} \times a_i} \pi_{\setminus i}(\cdot|o_{\setminus i}) \pi_i(\cdot|o_i) \log \frac{\pi_i(\cdot|o_i)}{\pi_i^k(\cdot|o_i)} da_{\setminus i} da_i \\
\iff & \int_{a_i} \pi_i(\cdot|o_i) \log \frac{\pi_i(\cdot|o_i)}{\pi_i^k(\cdot|o_i)} \left[\int_{a_{\setminus i}} \pi_{\setminus i}(\cdot|o_{\setminus i}) da_{\setminus i} \right] da_i \\
\iff & \int_{a_i} \pi_i(\cdot|o_i) \log \frac{\pi_i(\cdot|o_i)}{\pi_i^k(\cdot|o_i)} da_i \\
\iff & \text{KL}(\pi_i(\cdot|o_i), \pi_i^k(\cdot|o_i)).
\end{aligned}$$

We replace the original formula with the simplified one

$$\begin{aligned}
& \sum_{i=1}^n \left[\int_{\mathbf{o}} \mu(\mathbf{o}) \int_a \pi(\cdot|\mathbf{o}) \log \frac{\pi_i(\cdot|o_i)}{\pi_i^k(\cdot|o_i)} da d\mathbf{o} \right] < \varepsilon \\
\iff & \sum_{i=1}^n \left[\int_{\mathbf{o}} \mu(\mathbf{o}) \text{KL}(\pi_i(\cdot|o_i), \pi_i^k(\cdot|o_i)) d\mathbf{o} \right] < \varepsilon \\
\iff & \sum_{i=1}^n \left[\int_{\mathbf{o}} \mu(\mathbf{o}) \delta(o_i) d\mathbf{o} \right] < \varepsilon.
\end{aligned}$$

where we denote $\text{KL}(\pi_i(\cdot|o_i), \pi_i^k(\cdot|o_i))$ as $\delta(o_i)$. For the outer integral term, we have

$$\begin{aligned}
& \int_{\boldsymbol{o}} \mu(\boldsymbol{o}) \delta(o_i) d\boldsymbol{o} \\
\iff & \int_{o_{\setminus i} \times o_i} \mu(o_{\setminus i}) \mu(o_i) \delta(o_i) do_{\setminus i} do_i \\
\iff & \int_{o_i} \mu(o_i) \delta(o_i) \left[\int_{o_{\setminus i}} \mu(o_{\setminus i}) do_{\setminus i} \right] do_i \\
\iff & \int_{o_i} \mu(o_i) \delta(o_i) do_i \\
\iff & \mathbb{E}_{o_i \sim u_i} [\delta(o_i)].
\end{aligned}$$

Overall, we have

$$\begin{aligned}
& \mathbb{E}_{\boldsymbol{o} \sim \mu} [\text{KL}(\pi(\cdot|\boldsymbol{o}), \pi^k(\cdot|\boldsymbol{o}))] < \varepsilon \\
\iff & \sum_{i=1}^n \left[\int_{\boldsymbol{o}} \mu(\boldsymbol{o}) \int_a \pi(\cdot|\boldsymbol{o}) \log \frac{\pi_i(\cdot|o_i)}{\pi_i^k(\cdot|o_i)} da d\boldsymbol{o} \right] < \varepsilon \\
\iff & \sum_{i=1}^n \left[\int_{\boldsymbol{o}} \mu(\boldsymbol{o}) \delta(o_i) d\boldsymbol{o} \right] < \varepsilon \\
\iff & \sum_{i=1}^n \mathbb{E}_{o_i \sim u_i} [\delta(o_i)] < \varepsilon \\
\iff & \sum_{i=1}^n \mathbb{E}_{o_i \sim u_i} [\text{KL}(\pi_i(\cdot|o_i), \pi_i^k(\cdot|o_i))] < \varepsilon.
\end{aligned}$$

□

D Proof of Lemma Theorem 1

Proof.

$$\begin{aligned}
& D_{\text{KL}}(p(\mathbf{o}'|\mathbf{o}, a_i) \| q(\mathbf{o}'|\mathbf{o}, a_i)) \\
&= \int p(\mathbf{o}'|\mathbf{o}, a_i) \log \frac{p(\mathbf{o}'|\mathbf{o}, a_i)}{q(\mathbf{o}'|\mathbf{o}, a_i)} d\mathbf{o}' \\
&\leq \int \left(\int p(\mathbf{o}'|\mathbf{o}, a_i, a_{-i}) \pi_{\psi_{-i}}(a_{-i}|\mathbf{o}) da_{-i} \right) \\
&\quad \left(\log \int \frac{\pi_{\psi_{-i}}(a_{-i}|\mathbf{o})}{\pi_{\psi'_{-i}}(a_{-i}|\mathbf{o})} da_{-i} \right) d\mathbf{o}' \\
&\leq \int \left(\int \pi_{\psi_{-i}}(a_{-i}|\mathbf{o}) da_{-i} \right) \\
&\quad \left(\log \int \frac{\pi_{\psi_{-i}}(a_{-i}|\mathbf{o})}{\pi_{\psi'_{-i}}(a_{-i}|\mathbf{o})} da_{-i} \right) d\mathbf{o}' \\
&\leq \int \left(\log \int \frac{\pi_{\psi_{-i}}(a_{-i}|\mathbf{o})}{\pi_{\psi'_{-i}}(a_{-i}|\mathbf{o})} da_{-i} \right) d\mathbf{o}' \\
&\leq \log \int \left(\int \frac{\pi_{\psi_{-i}}(a_{-i}|\mathbf{o})}{\pi_{\psi'_{-i}}(a_{-i}|\mathbf{o})} da_{-i} \right) d\mathbf{o}' \\
&\propto \log \int \left(\int \log \frac{\pi_{\psi_{-i}}(a_{-i}|\mathbf{o})}{\pi_{\psi'_{-i}}(a_{-i}|\mathbf{o})} da_{-i} \right) d\mathbf{o}' \\
&\propto \log \int \left(\int \pi_{\psi_{-i}}(a_{-i}|\mathbf{o}) \log \frac{\pi_{\psi_{-i}}(a_{-i}|\mathbf{o})}{\pi_{\psi'_{-i}}(a_{-i}|\mathbf{o})} da_{-i} \right) d\mathbf{o}' \\
&= \log \int D_{\text{KL}}(\pi_{\psi_{-i}}(\mathbf{o}) \| \pi_{\psi'_{-i}}(\mathbf{o})) d\mathbf{o}' \\
&\propto D_{\text{KL}}(\pi_{\psi_{-i}}(\mathbf{o}) \| \pi_{\psi'_{-i}}(\mathbf{o})).
\end{aligned}$$

□

To explain the above proportional relationship more explicitly, let us consider such a simple Markov game. This Markov game contains a total of three states, an initial state s_0 and two end states s_1 and s_2 (here we assume that the agent can fully observe the state of the environment). There are 2 agents in total, and the size of each agent's action space is also 2, denoted as $A1 = \{a_{11}, a_{12}\}$ and $A2 = \{a_{21}, a_{22}\}$ respectively. In addition, we define the state transition probability and the policy of agent 2 as follows.

$$\begin{aligned}
p(s_1|a_{11}, a_{21}, s_0) &= 0.4, & p(s_2|a_{11}, a_{21}, s_0) &= 0.6, \\
p(s_1|a_{11}, a_{22}, s_0) &= 0.2, & p(s_2|a_{11}, a_{22}, s_0) &= 0.8, \\
p(s_1|a_{12}, a_{21}, s_0) &= 0.5, & p(s_2|a_{12}, a_{21}, s_0) &= 0.5, \\
p(s_1|a_{12}, a_{22}, s_0) &= 0.7, & p(s_2|a_{12}, a_{22}, s_0) &= 0.3, \\
\pi_2(a_{21}|s_0) &= m, & \pi_2(a_{22}|s_0) &= 1 - m, \\
\pi'_2(a_{21}|s_0) &= n, & \pi'_2(a_{22}|s_0) &= 1 - n,
\end{aligned}$$

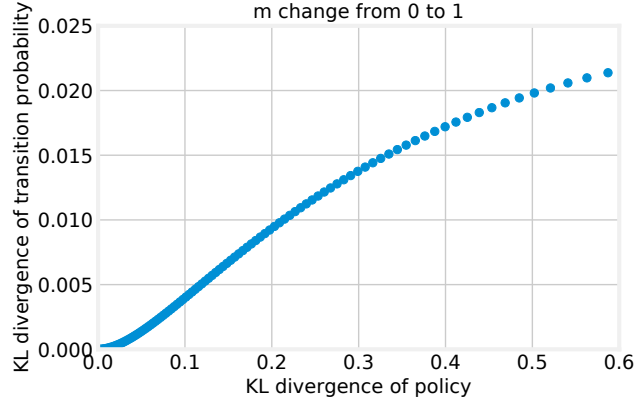


Figure 8: KL divergence of policy and KL divergence of transition probability on $0 < m < 1$.

where $n = m/2$ and $0 < n < m < 1$. If agent 1 takes action a_{11} on s_0 , then we have,

$$\begin{aligned}
& D_{\text{KL}}(p(s'|s_0, a_{11}) \| q(s'|s_0, a_{11})) \\
&= \sum p(s' | s_0, a_{11}) \log \frac{p(s' | s_0, a_{11})}{q(s' | s_0, a_{11})} \\
&= p(s_1 | s_0, a_{11}) \log \frac{p(s_1 | s_0, a_{11})}{q(s_1 | s_0, a_{11})} + \\
&\quad p(s_2 | s_0, a_{11}) \log \frac{p(s_2 | s_0, a_{11})}{q(s_2 | s_0, a_{11})} \\
&= (0.4m + 0.2(1-m)) \log \frac{0.4m + 0.2(1-m)}{0.4n + 0.2(1-n)} + \\
&\quad (0.6m + 0.8(1-m)) \log \frac{0.6m + 0.8(1-m)}{0.6n + 0.8(1-n)} \\
&= (0.2 + 0.2m) \log \frac{1+m}{1+n} + (0.8 - 0.2m) \log \frac{4-m}{4-n} \\
&= 0.2(1+m) \log \frac{2+2m}{2+m} + 0.2(4-m) \log \frac{8-2m}{8-m} \\
&= \log \left(\left(\frac{2+2m}{2+m} \right)^{0.2(1+m)} \left(\frac{8-2m}{8-m} \right)^{0.2(4-m)} \right),
\end{aligned}$$

and

$$\begin{aligned}
& D_{\text{KL}}(\pi_2(s_0) \| \pi'_2(s_0)) \\
&= \pi_2(a_{21}|s_0) \log \frac{\pi_2(a_{21}|s_0)}{\pi'_2(a_{21}|s_0)} + \pi_2(a_{22}|s_0) \log \frac{\pi_2(a_{22}|s_0)}{\pi'_2(a_{22}|s_0)} \\
&= m \log 2 + (1-m) \log \frac{2-2m}{2-m} \\
&= \log \left(2^m \left(\frac{2-2m}{2-m} \right)^{1-m} \right).
\end{aligned}$$

Draw the $D_{\text{KL}}(p(s'|s_0, a_{11}) \| q(s'|s_0, a_{11}))$ and $D_{\text{KL}}(\pi_2(s_0) \| \pi'_2(s_0))$ on $0 < m < 1$, we have Figure 8. We can see the proportional relationship between $D_{\text{KL}}(p(s'|s_0, a_{11}) \| q(s'|s_0, a_{11}))$ and $D_{\text{KL}}(\pi_2(s_0) \| \pi'_2(s_0))$ from the figure.

E Proof of Theorem 2

Proof.

$$\begin{aligned}
\text{KL}[\pi \mid \pi'] &= \int \int \pi(a_i, a_{-i} \mid \mathbf{o}) \log \frac{\pi(a_i, a_{-i} \mid \mathbf{o})}{\pi'(a_i, a_{-i} \mid \mathbf{o})} da_i da_{-i} \\
&= \int \int \pi(a_i \mid a_{-i}, \mathbf{o}) \pi(a_{-i} \mid \mathbf{o}) \\
&\quad \log \frac{\pi(a_i \mid a_{-i}, \mathbf{o}) \pi(a_{-i} \mid \mathbf{o})}{\pi'(a_i \mid a_{-i}, \mathbf{o}) \pi(a_{-i} \mid s)} da_i da_{-i} \\
&= \int \int \pi(a_i \mid a_{-i}, \mathbf{o}) \pi(a_{-i} \mid \mathbf{o}) \\
&\quad \left(\log \frac{\pi(a_i \mid a_{-i}, \mathbf{o})}{\pi'(a_i \mid a_{-i}, \mathbf{o})} + \log \frac{\pi(a_{-i} \mid \mathbf{o})}{\pi'(a_{-i} \mid s)} \right) da_i da_{-i} \\
&= \int \int \pi(a_i \mid a_{-i}, \mathbf{o}) \pi(a_{-i} \mid \mathbf{o}) \log \frac{\pi(a_i \mid a_{-i}, \mathbf{o})}{\pi'(a_i \mid a_{-i}, \mathbf{o})} da_i da_{-i} \\
&\quad + \int \int \pi(a_i \mid a_{-i}, \mathbf{o}) \pi(a_{-i} \mid \mathbf{o}) \log \frac{\pi(a_{-i} \mid \mathbf{o})}{\pi'(a_{-i} \mid \mathbf{o})} da_i da_{-i} \\
&= \int \int \pi(a_i \mid a_{-i}, \mathbf{o}) \pi(a_{-i} \mid \mathbf{o}) \log \frac{\pi(a_i \mid a_{-i}, \mathbf{o})}{\pi'(a_i \mid a_{-i}, \mathbf{o})} da_i da_{-i} + \\
&\quad \text{KL}[\pi_{-i} \mid \pi'_{-i}] \\
&= \int \text{KL}[\pi_i(a_{-i}, \mathbf{o}) \mid \pi'_i(a_{-i}, \mathbf{o})] \pi(a_{-i} \mid \mathbf{o}) da_{-i} \\
&\quad + \text{KL}[\pi_{-i} \mid \pi'_{-i}] \\
&\geq \text{KL}[\pi_{-i} \mid \pi'_{-i}].
\end{aligned}$$

So we have

$$\text{KL}[\pi \mid \pi'] \geq \frac{1}{n} \sum_i \text{KL}[\pi_{-i} \mid \pi'_{-i}].$$

□

F Trust Region decomposition Dilemma

In order to verify the existence of trust region decomposition dilemma, we defined a simple coordination environment. We extend the *Spread* environment of Section 6 to 3 agents and 3 landmarks, labeled **Spread-3**. We define different Markov random fields (see Figure 9) of the joint policy by changing the reward function of each agent.

Specifically, the reward function of each agent is composed of two parts, one is the minimum distance between all agents and the landmarks, and the other is collision. For the leftmost MRF in autoreffig:dilemma, all agents are independent of each other, that is, the reward function of each agent is only related to itself, only related to the minimum distance between itself and a certain landmark, and will not collide with other agents. We labeled this situation as **Spread-3-Sep**. For the middle MRF in autoreffig:dilemma, the reward function of agent j is the same as that of *Spread-3-Sep*, which is only related to itself; but agent i and k are interdependent. For agent i , its reward function consists of the minimum distance between i and k and the landmark, and whether the two collide. The reward function of agent k is similar. We labeled this situation as **Spread-3-Mix**. Finally, the rightmost MRF is consistent with the normal environment settings, labeled **Spread-3-Ful**.

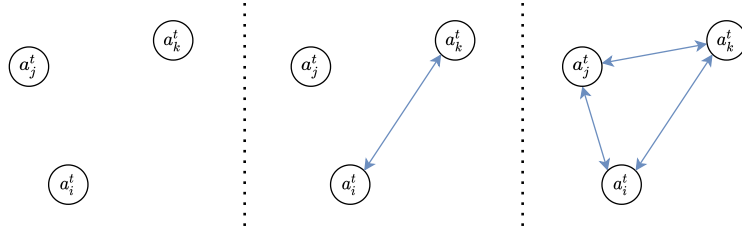


Figure 9: In the Spread-3 environment, 3 different Markov random fields are generated due to the different definition of the reward function of each agent. Note that these are not all possible Markov random fields, but three typical cases.

To verify the existence of trust region decomposition dilemma, we compare the performance of three different algorithms. First, we select MAAC without any trust region constraints as the baseline, labeled **MAAC**. Secondly, we choose MAMD based on mean-field approximation and naive trust region decomposition as one of the algorithms to be compared, labeled **MAMD**. Finally, we optimally assign trust region based on prior knowledge. For *Spread-3-Sep*, we do not impose any trust region constraints, same as *MAAC*; for *Spread-3-Mix*, we only impose equal size constraints on agent i and k ; and for *Spread-3-Ful*, we impose equal size constraints on all agents, same as *MAMD*. We labeled these optimally decomposition as **MAMD-OP**. The performance is shown in Figure 10.

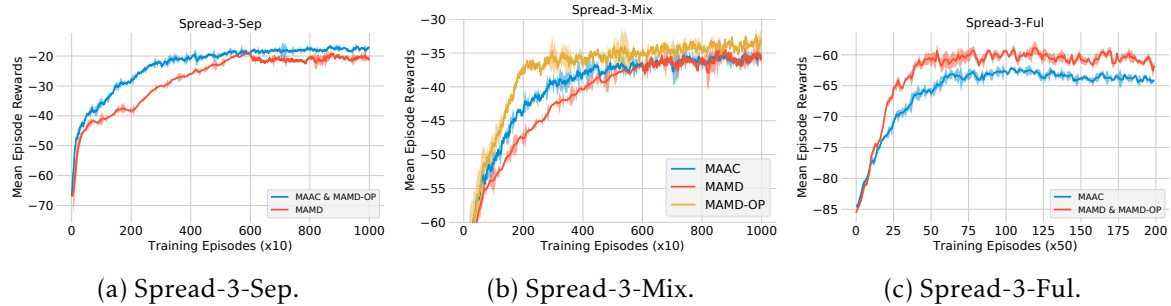


Figure 10: The performance of different trust region decomposition in different scenario. These results indicate the existence of trust region decomposition dilemma.

It can be seen from the figure that inappropriate decomposition of trust region will negatively affect the convergence speed and performance of the algorithm. The optimal decomposition method can make the algorithm performance and convergence speed steadily exceed baselines.

Note that the three algorithms compared here are all based on the MAAC with centralized critics. After we change the reward function of the agent, the information received by these centralized critics has more redundancy in some scenarios (for example, in *Spread-3-Sep* and *Spread-3-Mix*). To exclude the performance of the algorithm from being affected by these redundant information, we output the attention weights in MAAC, as shown in Figure 11. It can be seen from the figure that different algorithms can filter redundant information well, thus eliminating the influence of redundant information on the convergence speed and performance of the algorithm.

G Experimental Details

G.1 Environments

Spread. This environment (Lowe et al., 2017) has 2 agents, 2 landmarks. Each agents are globally rewarded based on how far the closest agent is to each landmark (sum of the minimum distances).

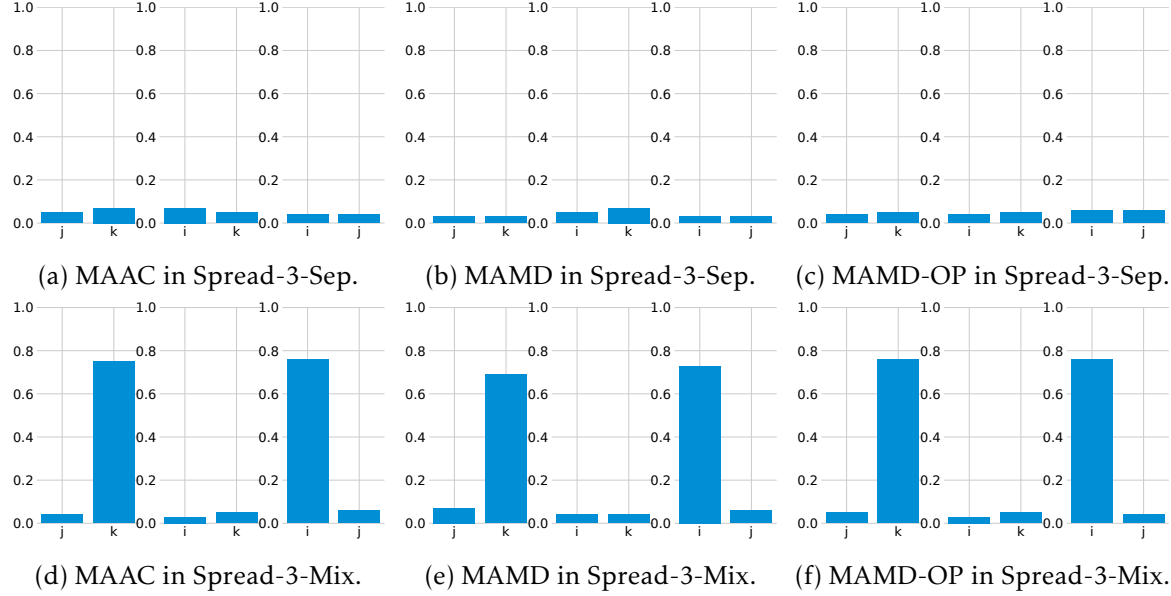


Figure 11: The attention weights of different agent of different trust region decomposition in different scenario. These results indicate the existence of trust region decomposition dilemma.

Locally, the agents are penalized if they collide with other agents (-1 for each collision).

Multi-Walker. In this environment (Terry et al., 2020), bipedal robots attempt to carry a package as far right as possible. A package is placed on top of 3 bipedal robots. A positive reward is awarded to each walker, which is the change in the package distance.

Rover-Tower. This environment (Iqbal & Sha, 2019) involves 8 agents, 4 of which are “rovers” and another 4 which are “towers”. At each episode, rovers and towers are randomly paired. The pair is negative rewarded by the distance of the rover to its goal. The rovers are unable to see in their surroundings and must rely on communication from the towers which can send one of 5 discrete messages.

Pursuit. 30 blue evaders and 8 red pursuer agents are placed in a grid with an obstacle. The evaders move randomly, and the pursuers are controlled (Terry et al., 2020). Every time the pursuers fully surround an evader each of the surrounding agents receives a reward of 5 and the evader is removed from the environment. Pursuers also receive a reward of 0.01 every time they touch an evader.

G.2 Network Architecture

Figure 12 shows the detailed parameters of the three main networks in the MAMT algorithm.

G.3 Hyperparameters

Table 1 shows the default configuration used for all the experiments of our methods (MAMD and MAMT) in this paper.

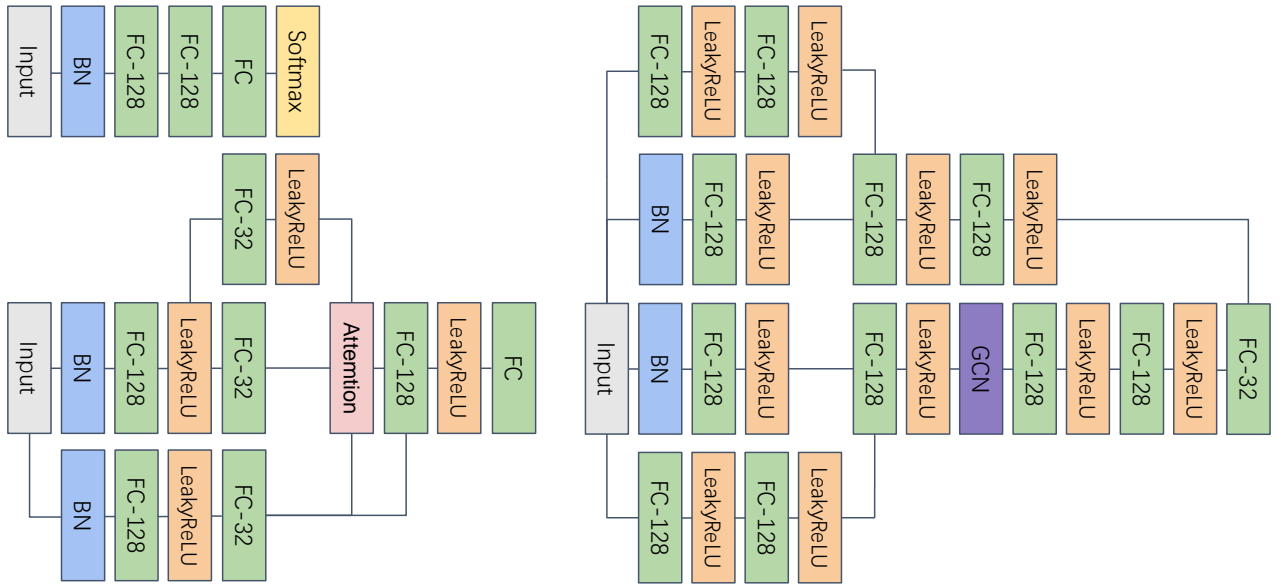


Figure 12: From top to bottom, from left to right, there are actor network (i.e. policy and modeling policy) architecture, critic network architecture, and trust region decomposition network architecture.

H More Results

Figure 13 to Figure 23 show the performance indicators of all agents in 4 environments under different random seeds.

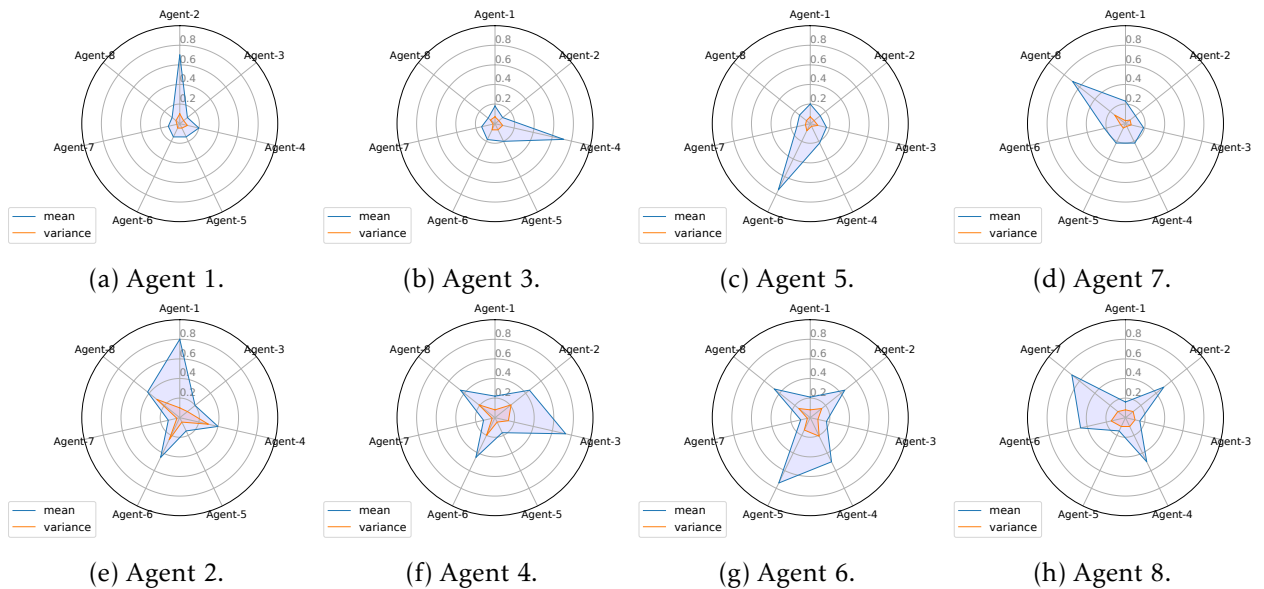


Figure 13: The mean and variance of coordination coefficient of each agent in *Rover-Tower* environment.

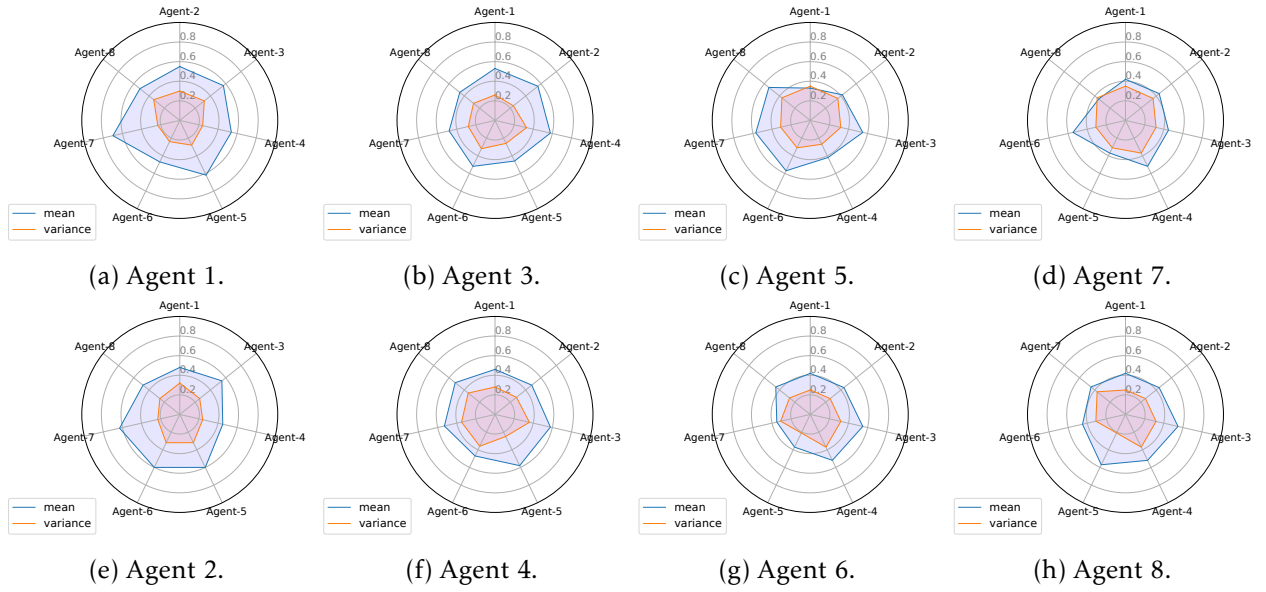


Figure 14: The mean and variance of coordination coefficient of each agent in *Pursuit* environment.

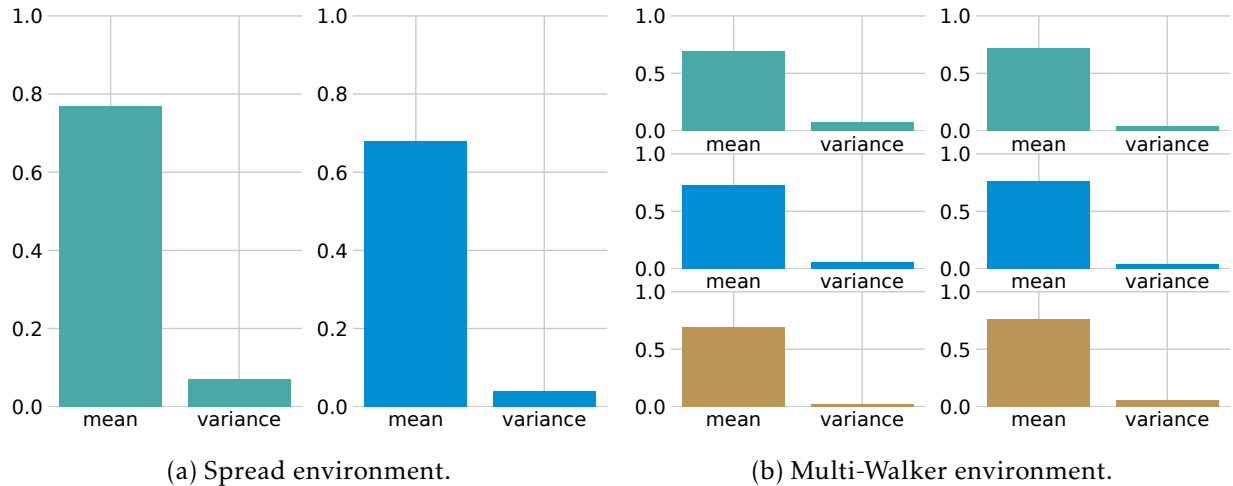


Figure 15: The mean and variance of coordination coefficient of each agent in *Spread* environment and *Multi-Walker* environment. Different color represents different agent.

Table 1: Default settings used in experiments.

Name	Default value
num parallel envs	12
step size	from 10,000 to 50,000
num epochs per step	4
steps per update	100
buffer size	1,000,000
batch size	1024
batch handling	Shuffle transitions
num critic attention heads	4
value loss	MSE
modeling policy loss	CrossEntropyLoss
discount	0.99
optimizer	Adam
adam lr	1e-3
adam mom	0.9
adam eps	1e-7
lr decay	0.0
policy regularization type	L2
policy regularization coefficient	0.001
modeling policy regularization type	L2
modeling policy regularization coefficient	0.001
critic regularization type	L2
critic regularization coefficient	1.0
critic clip grad	10 * num of agents
policy clip grad	0.5
soft reward scale	100
modeling policy clip grad	0.5
trust region decomposition network clip grad	10 * num of agents
trust region clip	from 0.01 to 100
num of iteration delay in mirror descent	100
tsallis q in mirror descent	0.2
δ in coordination coefficient	0.2

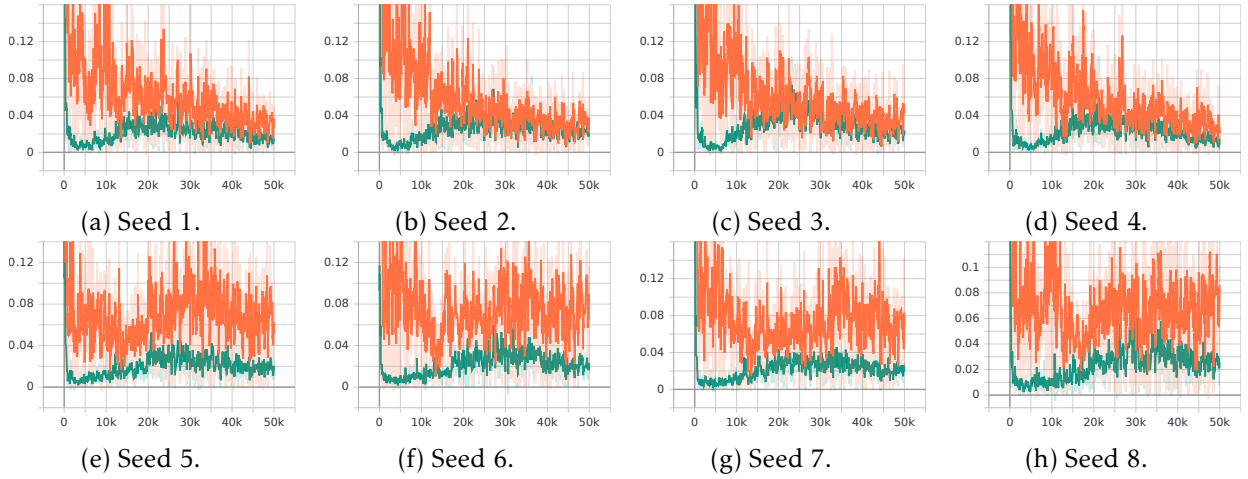


Figure 16: The averaged KL-divergence of each agent in *Rover-Tower* environments. Red line represents MAAC and green line represents MAMD-TRA.

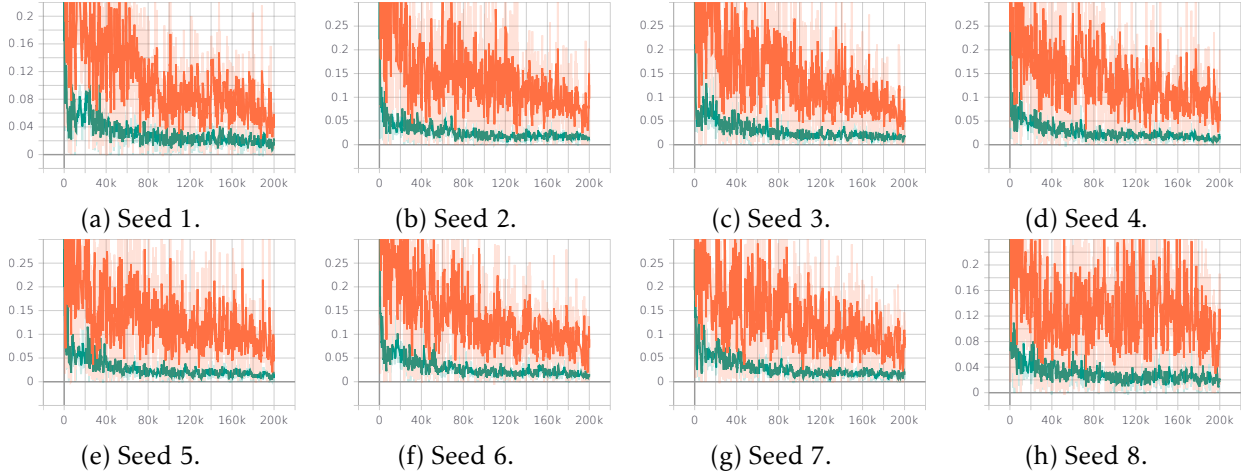


Figure 17: The averaged KL-divergence of each agent in *Pursuit* environments. Red line represents MAAC and green line represents MAMD-TRA.

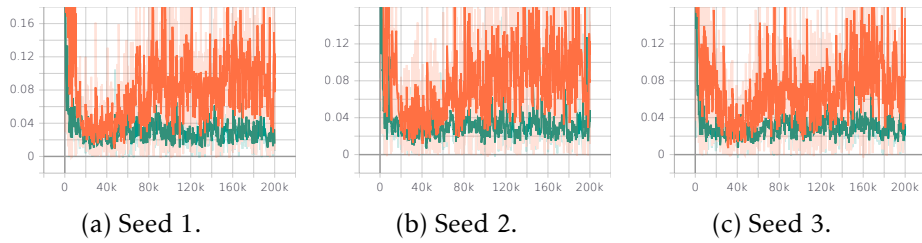


Figure 18: The averaged KL-divergence of each agent in *Multi-Walker* environments. Red line represents MAAC and green line represents MAMD-TRA.

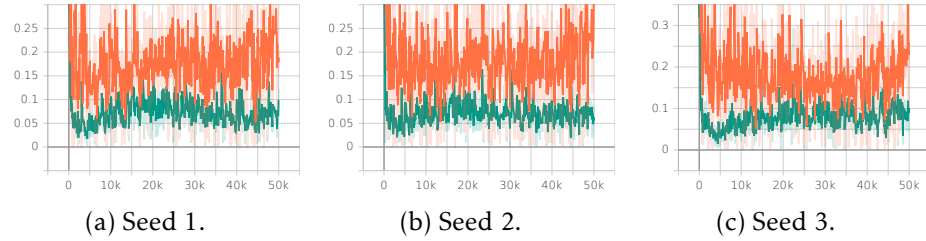


Figure 19: The averaged KL-divergence of each agent in *Spread* environments. Red line represents MAAC and green line represents MAMD-TRA.

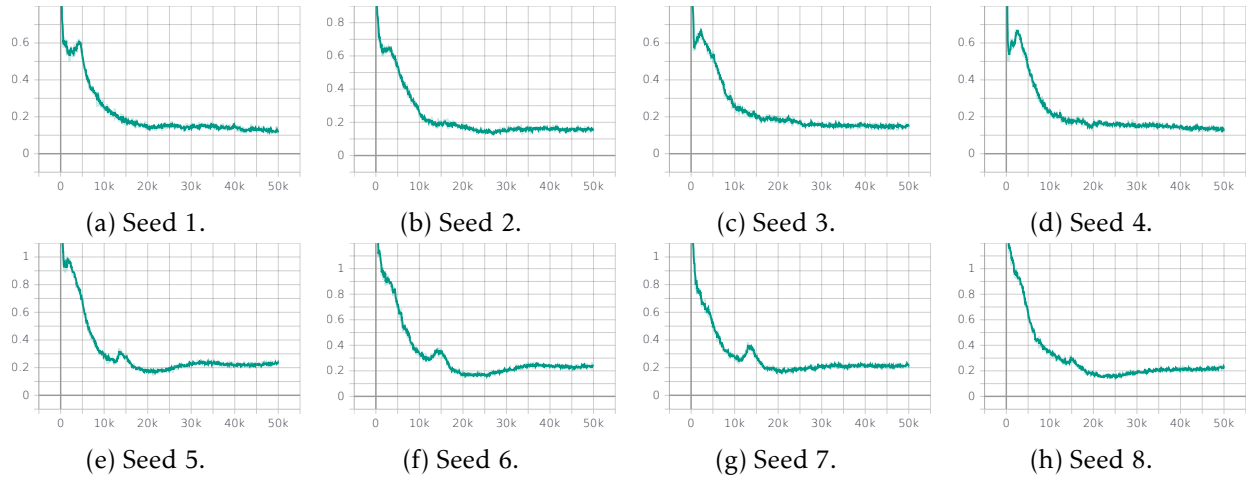


Figure 20: The averaged \hat{KL} of each agent in *Rover-Tower* environments.

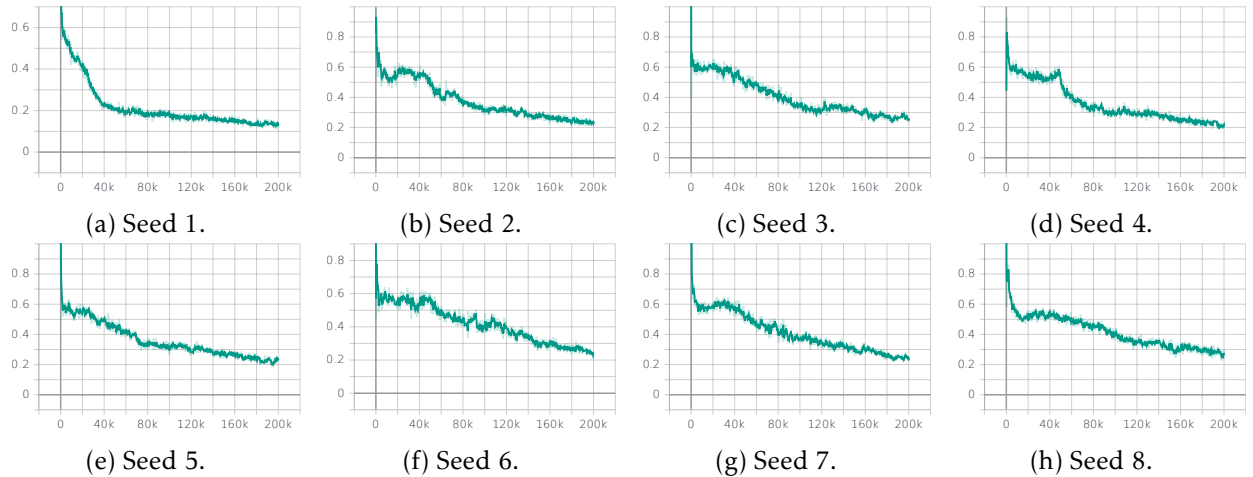


Figure 21: The averaged \hat{KL} of each agent in *Pursuit* environments.

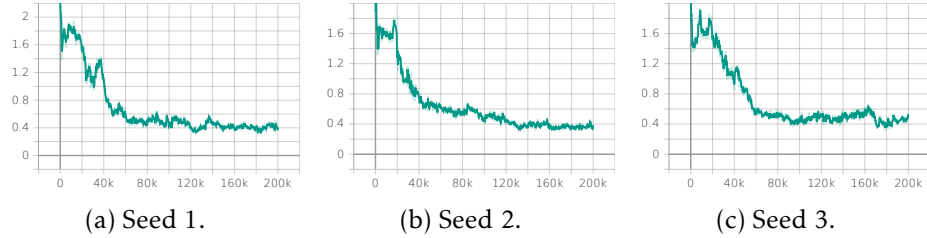


Figure 22: The averaged \hat{KL} of each agent in *Multi-Walker* environments.

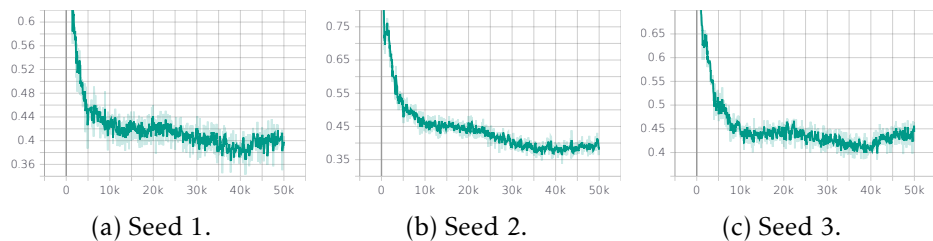


Figure 23: The averaged \hat{KL} of each agent in *Spread* environments.